

PREMA: Principled Tensor Data Recovery from Multiple Aggregated Views

Faisal M. Almutairi, Charilaos I. Kanatsoulis, and Nicholas D. Sidiropoulos

Abstract—Multidimensional data have become ubiquitous and are frequently involved in situations where the information is aggregated over multiple data atoms. The aggregation can be over time or other features, such as geographical location or group affiliation. We often have access to multiple aggregated views of the same data, each aggregated in one or more dimensions, especially when data are collected or measured by different agencies. However, data mining and machine learning models require detailed data for personalized analysis and prediction. Thus, data disaggregation algorithms are becoming increasingly important in various domains. The goal of this paper is to reconstruct finer-scale data from multiple coarse views, aggregated over different (subsets of) dimensions. The proposed method, called PREMA, leverages low-rank tensor factorization tools to provide recovery guarantees under certain conditions. PREMA is flexible in the sense that it can perform disaggregation on data that have missing entries, i.e., partially observed. The proposed method considers challenging scenarios: i) the available views of the data are aggregated in two dimensions, i.e., double aggregation, and ii) the aggregation patterns are unknown. Experiments on real data from different domains, i.e., sales data from retail companies, crime counts, and weather observations, are presented to showcase the effectiveness of PREMA.

Index Terms—Data disaggregation, tensor decomposition, multiview data.



1 INTRODUCTION

DATA aggregation is the process of summing (or averaging) multiple data samples from a certain dataset, which results in data resolution reduction and compression. The most common type of aggregation is *temporal aggregation*. For example, the annual income is the aggregate of the monthly salary. Aggregation over other attributes is also common, e.g., data get aggregated geographically (e.g., population of New York) or according to a defined affiliation (e.g., Computer Science students). The latter is known in economics as *contemporaneous aggregation* [1]. The different types of aggregation are often combined, e.g., the number of foreigners who visited different US states in 2018 can be aggregated in time, location (states), and affiliation (nationality).

Data aggregation serves multiple objectives, the most important being data summarization. In particular aggregated data enjoy concise representations, which is pivotal in the era of data deluge. Aggregation also benefits various other purposes, including scalability [2], communication cost [3], and privacy [4]. In some cases, the lack of data collection in finer granularity, either in time or attribute of elements, is the reason why we find the data as aggregates. For example, in the energy disaggregation research problem, the total household power consumption readings are seen as aggregates of their constituent device-level consumption. Aggregated data are common in a wide range of domains, such as economics, health care [5], education [6], wireless

communication, signal and image processing, databases [7], and smart grid systems [8].

Unfortunately, the favorable properties of data aggregation come with major shortcomings. A plethora of data mining and machine learning tasks strive for data in finer granularity (disaggregated), thus data aggregation is undesirable. Along the same lines, algorithms designed for personalized analysis and accurate prediction significantly benefit from enhanced data resolution. Analysis results can differ substantially when using aggregated versus disaggregated data. Particularly, studies in the field of economics show that data aggregation results in information loss and misleading conclusions at the individual-level [9], [10]. Furthermore, in supply chain management, researchers have concluded that aggregating sales over time, products, or locations has a negative impact on demand forecasting [11]. On the other hand, disaggregation prior to analysis is very effective in environmental studies [12], and leads to richer findings in learning analytics [13].

The previous discussion reveals a clear *trade-off* between the need for data aggregation and the benefit of disaggregated data. This has motivated numerous works in developing algorithms for data disaggregation. In general, the task of data disaggregation is an inverse ill-posed problem. In order to handle the problem, classic techniques exploit side information or domain knowledge, in their attempt to make the problem overdetermined and consequently enhance the disaggregation accuracy. Some common prior models, imposed on the target higher resolution data, involve smoothness, periodicity [14], and non-negativity plus sparsity over a given dictionary [15]. Such prior constraints are invoked when no other information is available about the data to be disaggregated.

An interesting question arises when a dataset is aggregated over more than one dimension. This is a popular

- F. M. Almutairi and C. I. Kanatsoulis are with the Department of Electrical and Computer Engineering, University of Minnesota, Minneapolis, MN 55455 USA.
E-mails: (almut012, kanat003)@umn.edu.
- N. D. Sidiropoulos is with the Department of Electrical and Computer Engineering, University of Virginia, Charlottesville, VA 22903, USA.
E-mail: nikos@virginia.edu

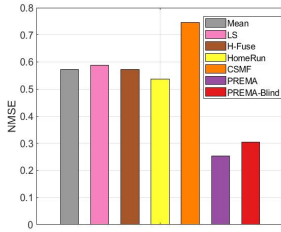


Fig. 1: PREMA is effective with real data.

research problem in the area of business and economics going back to the 70’s [16], [17]. In this case temporal *and* contemporaneous aggregated data are available [18], and algorithms have been developed to integrate them in the disaggregation process. For instance, given a country consisting of regions, we are interested in estimating the quarterly gross regional product (GRP) values, given the annual GRP per region (temporal aggregate) *and* the quarterly national series (contemporaneous aggregate) [19]. Similarly, in retail supply chains two sources of data are available to top suppliers: 1) historical *orders* from the retailers’ Distribution Centers (DC orders), aggregated over their multiple stores; and 2) Point of Sale (POS) data at the store level, commonly aggregated in time. In particular, DC order data are immediately available to suppliers, whereas the POS data are owned by the retailers. Both DC and POS data are used to forecast demand, and especially POS data are vital in predicting future orders [20]. For that reason, many retailers share POS with their suppliers to assist in forecasting orders and avoid shortage in inventory [21]. Another notable example appears in healthcare, where data are collected by national, regional, and local government agencies, health and scientific organizations, insurance companies and other entities, and are often aggregated in many dimensions (e.g., temporally, geographically, or group of hospitals), often to preserve privacy [5].

Algorithms designed to disaggregate data with two different aggregates fuse the available observations by assuming autoregressive models and adopting Least Squares (LS) criteria [18], [19]. However, it is unclear whether the assumed models are identifiable, i.e., an optimal solution of the model is not guaranteed to be the true disaggregated dataset. The general disaggregation problem is ill-posed, which is clearly undesirable. Identifiability guarantees are important, in the sense of assuring correct recovery under certain reasonable conditions. In our present context, identifiability has not received the attention it deserves, likely because guaranteed recovery is considered mission impossible under realistic conditions. With multiview data aggregated in different ways, however, the problem can be well-posed, as we will show in this paper.

Our work is inspired by the following question: *Is the disaggregation task possible when the data are: 1) multidimensional, and 2) observed by different agencies via diverse aggregation mechanisms?* This is a well motivated problem due to the ubiquitous presence of data with multiple dimensions (three or more), also known as tensors, in a large number of applications. Also it is very common that aggregation happens in more than one dimensions of *the same data* as in

the previously explained examples.

The informal definition of the problem is given as follows:

Informal Problem 1 (Multidimensional Disaggregation).

- **Given:** two (or more) observations of a multidimensional dataset, each represents a view of the data aggregated in one dimension (e.g., temporal and contemporaneous aggregates).
- **Recover:** the data in higher resolution (disaggregated) in all the dimensions.

We propose PREMA: a framework for fusing the multiple aggregates of multidimensional data. The proposed approach represents the target high resolution data as a *tensor*, and models them using the *canonical polyadic decomposition* (CPD) to reduce the number of unknowns, while capturing correlations and higher-order statistical dependencies across dimensions. PREMA employs a coupled CPD approach and estimates the low-rank factors of the target data, to perform the disaggregation task. This way the originally ill-posed disaggregation problem is transformed to an overdetermined one, by leveraging the uniqueness properties of the CPD. PREMA is flexible in the sense that it can disaggregate partially observed data, i.e., data with missing entries. This is practically important as partially observed data commonly appear in real-world applications. A common practise in machine learning is setting missing values as zeros, to avoid the complication they bring to the solution. However, this results in noisy data and negatively impact the disaggregation accuracy in our context. PREMA takes into account several well-known challenges that emerge in real-life databases: the available measurements can have different scales within one aggregate (e.g., mixed monthly and yearly aggregates), and gaps in the timeline of the aggregated measurements (i.e., periods with no value reported). Moreover, we propose an algorithm (called B-PREMA) that handles the disaggregation task in cases where the aggregation pattern is unknown. Furthermore, the proposed framework not only provides a disaggregation algorithm, but it can give insights that can be potentially exploited in creating accurately retrievable data summaries for database applications. Conversely, our work provides insights on when aggregation does not preserve anonymity.

We evaluated PREMA on real data from different domains, i.e., sales data from retail companies, crime counts, and weather observations. Experimental results show that the proposed algorithm reduces the disaggregation error of the best baseline by up to 75%. Figure 1 shows the disaggregation error in terms of the Normalized Mean Square Error (NMSE) of PREMA and the baselines with real data of the weekly sales of items in different stores of a retail company (CRA dataset, described in Section 4.1). We are given two observations: 1) the weekly sales are available as monthly aggregates, and 2) the weekly sales are aggregated over groups of stores (94 stores are geographically divided into 18 area). PREMA outperforms all the competitors, even if the disaggregation pattern is unknown (B-PREMA)—all the baselines use the aggregation information. The fact that the naive mean (Mean) gives a large error, indicates that the

data are not smooth and task is difficult. In summary, the contributions of our work are as follows:

- **Formulation:** we formally define the multidimensional data disaggregation task from multiple views, aggregated across different dimensions, and provide an efficient algorithm.
- **Identifiability:** the considered model can provably transform the original ill-posed disaggregation problem to an identifiable one.
- **Effectiveness:** PREMA recovers data with large improvement in the accuracy of the best baseline on real data, even without any knowledge of the aggregation mechanism.
- **Scalability:** PREMA scales linearly with the data size in terms of run time.
- **Unknown aggregation:** the proposed model works even when the aggregation mechanism is unknown.
- **Flexibility :** PREMA can disaggregate partially observed data.

The paper is structured as follows. We explain the needed background and the related work in Section 2, and introduce our proposed method in Section 3. Then, we explain our experimental setup in Section 4 and show the experimental results in Section 5. Finally, we summarize conclusions and take-home points in Section 6.

2 BACKGROUND & RELATED WORK

In this section, we review some tensor algebraic tools utilized by the proposed framework, define the disaggregation problem, and provide an overview of the related work. Table 1 summarizes the main symbols and operators used throughout the paper.

2.1 Tensor Algebra

Tensors are multidimensional arrays indexed by three or more indices, (i, j, k, \dots) . A third-order tensor $\underline{\mathbf{X}} \in \mathbb{R}^{I \times J \times K}$ consists of three modes: rows $\underline{\mathbf{X}}(:, j, k)$, columns $\underline{\mathbf{X}}(i, :, k)$, and fibers $\underline{\mathbf{X}}(i, j, :)$. Moreover, $\underline{\mathbf{X}}(i, :, :)$, $\underline{\mathbf{X}}(:, j, :)$, and $\underline{\mathbf{X}}(:, :, k)$ denote the i^{th} horizontal, j^{th} lateral, and k^{th} frontal slabs of $\underline{\mathbf{X}}$, respectively.

Tensor decomposition (CPD/PARAFAC): The outer product of two vectors $(\mathbf{a} \circ \mathbf{b})$ results in a rank-one matrix. A rank-one third-order tensor $\underline{\mathbf{X}} \in \mathbb{R}^{I \times J \times K}$ is an outer product of three vectors: $\underline{\mathbf{X}}(i, j, k) = \mathbf{a}(i)\mathbf{b}(j)\mathbf{c}(k)$, $\forall i \in \{1, \dots, I\}$, $j \in \{1, \dots, J\}$, and $k \in \{1, \dots, K\}$, i.e., $\underline{\mathbf{X}} = (\mathbf{a} \circ \mathbf{b} \circ \mathbf{c})$, where $\mathbf{a} \in \mathbb{R}^I$, $\mathbf{b} \in \mathbb{R}^J$, and $\mathbf{c} \in \mathbb{R}^K$. The Canonical Polyadic Decomposition (CPD) (also known as PARAFAC) of a third-order tensor $\underline{\mathbf{X}} \in \mathbb{R}^{I \times J \times K}$ decomposes it into a sum of R rank-one tensors [22], i.e.,

$$\underline{\mathbf{X}} = \sum_{r=1}^R \mathbf{a}_r \circ \mathbf{b}_r \circ \mathbf{c}_r \quad (1)$$

where R is the *tensor rank* and represents the minimum number of outer products needed, and $\mathbf{a}_r \in \mathbb{R}^I$, $\mathbf{b}_r \in \mathbb{R}^J$, and $\mathbf{c}_r \in \mathbb{R}^K$. For brevity, we use $\underline{\mathbf{X}} = \llbracket \mathbf{A}, \mathbf{B}, \mathbf{C} \rrbracket$ to denote the relationship in (1). $\mathbf{A} \in \mathbb{R}^{I \times R}$, $\mathbf{B} \in \mathbb{R}^{J \times R}$, and $\mathbf{C} \in \mathbb{R}^{K \times R}$ are the factor matrices with columns \mathbf{a}_r , \mathbf{b}_r , and

\mathbf{c}_r respectively, i.e., $\mathbf{A} = [\mathbf{a}_1 \ \mathbf{a}_2 \ \dots \ \mathbf{a}_R]$ and likewise for \mathbf{B} and \mathbf{C} .

CPD uniqueness: An important property of the CPD is that \mathbf{A} , \mathbf{B} , \mathbf{C} are essentially unique under mild conditions. CPD identifiability is established by the following theorem:

Theorem 1. [23] Let $\underline{\mathbf{X}} = \llbracket \mathbf{A}, \mathbf{B}, \mathbf{C} \rrbracket$ with $\mathbf{A} : I \times R$, $\mathbf{B} : J \times R$, and $\mathbf{C} : K \times R$. Assume that \mathbf{A} , \mathbf{B} and \mathbf{C} are drawn from some joint absolutely continuous distribution. Also assume $I \geq J \geq K$ without loss of generality. If $R \leq \frac{1}{16}JK$, then the decomposition of $\underline{\mathbf{X}}$ in terms of \mathbf{A} , \mathbf{B} , and \mathbf{C} is essentially unique, almost surely.

Essential uniqueness means that \mathbf{A} , \mathbf{B} , \mathbf{C} are unique up to common column permutation and scaling/ counter-scaling.

The CPD is also essentially unique, even if the tensor is incomplete (has missing entries). Several works have been proposed to establish CPD identifiability of tensors with missing entries and consider fiber sampled [24], regularly sampled [25] or randomly sampled tensors [26]. The conditions for uniqueness are in general stricter compared to the case where the full tensor is available.

Tensor matricization (unfolding): There are three different ways to unfold (obtain a matrix view of) a third-order tensor $\underline{\mathbf{X}}$ of size $I \times J \times K$. First, the mode-3 unfolding is obtained by the vectorization and parallel stacking of the frontal slabs $\underline{\mathbf{X}}(:, :, k)$ as follows [27]

$$\mathbf{X}_3 = [\text{vec}(\underline{\mathbf{X}}(:, :, 1)), \dots, \text{vec}(\underline{\mathbf{X}}(:, :, K))] \in \mathbb{R}^{I \times JK} \quad (2)$$

Equivalently, we can express \mathbf{X}_3 using the CPD factor matrices as $\mathbf{X}_3 = (\mathbf{B} \odot \mathbf{A})\mathbf{C}^T$. In the same vein, we may consider horizontal slabs to express the matricization over the first mode

$$\begin{aligned} \mathbf{X}_1 &:= [\text{vec}(\underline{\mathbf{X}}(1, :, :)), \dots, \text{vec}(\underline{\mathbf{X}}(I, :, :))] \\ &= (\mathbf{C} \odot \mathbf{B})\mathbf{A}^T \in \mathbb{R}^{JK \times I} \end{aligned} \quad (3)$$

or lateral slabs to obtain mode-2 unfolding

$$\begin{aligned} \mathbf{X}_2 &:= [\text{vec}(\underline{\mathbf{X}}(:, 2, :)), \dots, \text{vec}(\underline{\mathbf{X}}(:, J, :))] \\ &= (\mathbf{C} \odot \mathbf{A})\mathbf{B}^T \in \mathbb{R}^{IK \times J} \end{aligned} \quad (4)$$

Mode product: It is the operation of multiplying a matrix to a tensor in one particular mode, e.g., mode-1 product of matrix $\mathbf{U} \in \mathbb{R}^{I_u \times I}$ and tensor $\underline{\mathbf{X}} \in \mathbb{R}^{I \times J \times K}$ corresponds to multiplying \mathbf{U} to every column $\underline{\mathbf{X}}(i, :, k)$ of the tensor [28]. Similarly, mode-2 (mode-3) product corresponds to multiplying a matrix by every row (fiber) of $\underline{\mathbf{X}}$. Applying mode-1, mode-2, and mode-3 products to a third-order tensor $\underline{\mathbf{X}} \in \mathbb{R}^{I \times J \times K}$ jointly is represented using the following notation:

$$\underline{\mathbf{Y}} = \underline{\mathbf{X}} \times_1 \mathbf{U} \times_2 \mathbf{V} \times_3 \mathbf{W} \in \mathbb{R}^{I_u \times J_v \times K_w} \quad (5)$$

where “ \times_i ” denotes the product over the i^{th} mode, $\mathbf{U} \in \mathbb{R}^{I_u \times I}$, $\mathbf{V} \in \mathbb{R}^{J_v \times J}$, and $\mathbf{W} \in \mathbb{R}^{K_w \times K}$. Mode-1 multiplication results in reducing the tensor size in the first dimension if $(I_u < I)$, similarly with the other modes. Moreover, if rows of \mathbf{U} are binary vectors with more than one 1, then each horizontal slab of $\underline{\mathbf{Y}}$ is a sum of horizontal slabs of $\underline{\mathbf{X}}$ that correspond to the 1's in a particular row in \mathbf{U} . In the same vein, \mathbf{V} and \mathbf{W} could aggregate the lateral and frontal slabs, respectively; see Fig. 2. The mode product is

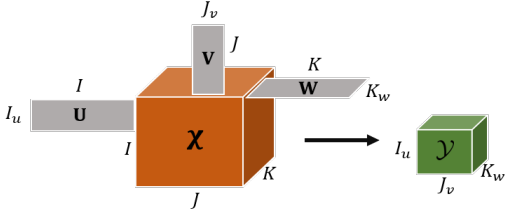


Fig. 2: Illustration of mode product with $(I_u < I)$, $(J_v < J)$, and $(K_w < K)$.

TABLE 1: Symbols and Definitions

Symbol	Definition
$\mathbf{x}, \mathbf{X}, \underline{\mathbf{X}}$	Vector, matrix, tensor
\mathbf{X}_i	Mode- i matricization (unfolding)
$\ \cdot\ _F$	Frobenius norm of tensor
\mathbf{A}^T	Transpose of matrix \mathbf{A}
$\text{vec}(\mathbf{A})$	Vectorization operator for matrix \mathbf{A}
\circ	Outer product
$[\cdot]$	Kruskal operator, e.g., $\underline{\mathbf{X}} \approx [\mathbf{A}, \mathbf{B}, \mathbf{C}]$
\otimes	Kronecker product
\odot	Khatri-Rao product (column-wise Kronecker)
\otimes	Hadamard (elementwise) product

also reflected in the CPD of the tensor, i.e., the operation in (5), when $\underline{\mathbf{X}} = [\mathbf{A}, \mathbf{B}, \mathbf{C}]$, results in: $\underline{\mathbf{Y}} = [\mathbf{U}\mathbf{A}, \mathbf{V}\mathbf{B}, \mathbf{W}\mathbf{C}]$

2.2 Disaggregation Problem

The goal of the disaggregation task is to estimate a particular series in a higher resolution, given observations in lower resolution. In this subsection we present a high level linear algebraic view of disaggregation. This reveals the challenge of the task, which is the relationship between equations versus unknowns—detailed analysis follows in the next section.

In the disaggregation problem, we are given a set of measurements $\mathbf{y} \in \mathbb{R}^{I_u}$ aggregated over the dataset $\mathbf{x} \in \mathbb{R}^I$ and our goal is to find \mathbf{x} . This can be cast as a linear inverse problem $\mathbf{y} = \mathbf{U}\mathbf{x}$, where $\mathbf{U} \in \mathbb{R}^{I_u \times I}$ is a ‘fat’ *aggregation matrix* that maps the measurements and the variables as in the illustrative example below.

$$\underbrace{\begin{bmatrix} 1 & 1 & 0 & 0 & 0 \\ 0 & 0 & 0 & 1 & 1 \\ 0 & 1 & 1 & 0 & 0 \end{bmatrix}}_{\mathbf{U}} \times \underbrace{\begin{bmatrix} x_1 \\ x_2 \\ x_3 \\ x_4 \\ x_5 \end{bmatrix}}_{\mathbf{x}} = \underbrace{\begin{bmatrix} y_1 \\ y_2 \\ y_3 \end{bmatrix}}_{\mathbf{y}} \quad (6)$$

In practical settings, the number of available aggregated measurements is much smaller than the number of variables (i.e., $I_u \ll I$), resulting in an under-determined, ill-posed problem. This is the major challenge of disaggregation, even when more than one aggregates are available. In real databases, the measurements can have overlaps (e.g., y_1 and y_3 in (6)) or gaps (e.g., y_1 and y_2).

In this work, we consider the case where multidimensional data (tensors) are aggregated over different dimensions. Let $\underline{\mathbf{X}} \in \mathbb{R}^{I \times J \times K}$ be the target high resolution third-order tensor. Instead we observe sets of measurements, each aggregated over one dimension. For example, $\underline{\mathbf{Y}} \in \mathbb{R}^{I_u \times J \times K}$, where $I_u \ll I$, if the aggregation is over the first mode (dimension). Then, the mapping in (6) involves the

columns of the target disaggregated tensor. In other words, $\underline{\mathbf{Y}}$ is the result of mode-1 product of the aggregation matrix \mathbf{U} and $\underline{\mathbf{X}}$. The same idea applies when the aggregation is over the second or third mode. A more challenging case appears when one of the available observations is aggregated over more than one mode/dimension (e.g., $\underline{\mathbf{Y}} \in \mathbb{R}^{I \times J_v \times K_w}$, where $J_v \ll J$ and $K_w \ll K$). For instance, sales are reported for categories rather than individual items in groups of stores. This is a double aggregation over stores and items and the proposed method can work under such challenging scenarios.

2.3 Related Work

Data disaggregation and fusion: The problem of data integration and fusion [29], [30] from multiple sources has attracted the attention of several communities, due to the increasing access to all kinds of data, especially in database applications. A very challenging task in data integration, is that of recovering a sequence of events (e.g., time series) from multiple aggregated reports [15], [31], [32]. A common approach is to formulate the problem as linear LS as in (6). In practice, however, the number of available aggregated samples is often significantly smaller than the length of the target series, resulting in an under-determined system of equations. To resolve this, previous algorithms have employed Tikhonov regularization to the ill-posed problem to impose some domain knowledge constraints, e.g., smoothness and periodicity [14].

Fusing multiple observations of a dataset, aggregated in different dimensions (e.g., temporal and contemporaneous), for disaggregation purposes, is a well studied task in the field of finance and economics [16], [17], [18], [19], [33]. The considered approaches try to exploit linear relations between the target series in high resolution and the available aggregated measurements. However, it is unclear whether the assumed models are identifiable, i.e, the model is not guaranteed to disaggregate the data. On the top of that, application specific assumptions are imposed, which require additional information to perform disaggregation.

(Coupled) tensor factorization: Time series analysis, for various applications, is moving towards modern high-dimensional methods. For example, matrix and tensor factorization have been used in demand forecasting [34], mining and information extraction from complex time-stamped series [35], and prediction of unknown locations in spatio-temporal data [36].

Data share common dimension(s) in a wide spectrum of applications. In such cases, coupled factorization techniques are commonly used to fuse the information for prediction [37] and learning. In recommender systems, for example, we have (user \times item \times time) *and* (user \times features). In this case, the tensor and the features matrix are coupled in the user mode [38]. Coupled tensor factorization has also been proposed for image processing [39], remote sensing [40], [41] and medical imaging problems [25], [42]. The work in [41], for example, employs a coupled CPD model to fuse a hyperspectral image with a multispectral image, in order to produce a high spatial and spectral resolution image.

To our knowledge, this work is the first that proposes a coupled tensor factorization approach to tackle data disaggregation applications.

3 PROPOSED FRAMEWORK: PREMA

Multidimensional data are indexed by multiple indices, e.g., (i, j, k) . Therefore, it can naturally be represented as a tensor $\underline{\mathbf{X}} \in \mathbb{R}^{I \times J \times K}$. The different modes represent the physical dimensions of the data (e.g., time stamps, locations, items, users). For the sake of simplicity of exposition, we focus on three-dimensional data in our formulation and algorithm. However, the proposed framework can handle more general cases with data of higher dimensions.

In the remaining of this section, we give a detailed description and analysis of PREMA. Particularly, we explain the proposed model in Section 3.1, formulate PREMA in Section 3.2, and present the derived algorithm in Section 3.3. The complexity of PREMA is discussed in Section 3.4. Identifiability of PREMA is discussed in section 3.5. Finally, B-PREMA is introduced in Section 3.6, which handles the disaggregation when the aggregation matrices are unknown.

3.1 Problem & Model Overview

Multidimensional aggregation is common when data are collected or released by different agencies, resulting in multiple views of the same dataset. We will explain the concept with the example of retail sales which we use in the experiments. Estimating the retail sales in higher resolution, enables accurate planning of more economically efficient commerce. However, the number of sold items is often collected/aggregated over a longer period of time (e.g., monthly) at the store-level (temporal aggregate $\underline{\mathbf{Y}}^t$). Another source is usually available (e.g., suppliers, or manufacturers) that provides information about the number of the same items in finer time scale. However, this source is aggregated over groups of stores, e.g., based on their geographical location or affiliation to a company (contemporaneous aggregate $\underline{\mathbf{Y}}^c$). In a more restricted scenario, the second source might collect information about each category of items rather than each item individually. Oftentimes, data are partially observed, i.e., have missing entries. In our example, not all items are offered in all stores during all the considered time stamps.

Formally, we are interested in the following:

Problem 1 (Multidimensional Disaggregation).

- **Given** two aggregated views of three-dimensional series $\underline{\mathbf{X}} \in \mathbb{R}^{I \times J \times K}$; $\underline{\mathbf{Y}}^t \in \mathbb{R}^{I \times J \times K_w}$, and $\underline{\mathbf{Y}}^c \in \mathbb{R}^{I_u \times J \times K}$ (or $\underline{\mathbf{Y}}^c \in \mathbb{R}^{I_u \times J_v \times K}$), with $I_u < I$, $J_v < J$, and $K_w < K$, and possibly missing entries.
- **Recover** the original disaggregated multidimensional data $\underline{\mathbf{X}} \in \mathbb{R}^{I \times J \times K}$.

Note that each aggregated observation is the result of mode product of the target series with an aggregation matrix. In particular $\underline{\mathbf{Y}}^t = \underline{\mathbf{X}} \times_3 \mathbf{W}$, where $\mathbf{W} \in \mathbb{R}^{K \times K_w}$ is an aggregation matrix with $K_w < K$, and $\underline{\mathbf{Y}}^c = \underline{\mathbf{X}} \times_1 \mathbf{U}$, where $\mathbf{U} \in \mathbb{R}^{I \times I_u}$ is an aggregation matrix with $I_u < I$. In the case where one view is jointly aggregated in 2 dimensions, e.g., sales are aggregated over group of stores and group of items, $\underline{\mathbf{Y}}^c = \underline{\mathbf{X}} \times_1 \mathbf{U} \times_2 \mathbf{V}$, where $\mathbf{V} \in \mathbb{R}^{J \times J_v}$ is an aggregation matrix with $J > J_v$.

PREMA aims to fuse the different available aggregates in order to estimate the multidimensional series in the desired

higher resolution. At a higher level, the main idea behind the proposed method is that the target multidimensional series, $\underline{\mathbf{X}} \in \mathbb{R}^{I \times J \times K}$, admits a CPD model. Therefore, it can be well approximated using its CPD factors $\mathbf{A}, \mathbf{B}, \mathbf{C}$ (i.e., $\underline{\mathbf{X}} \approx \llbracket \mathbf{A}, \mathbf{B}, \mathbf{C} \rrbracket$). Exploiting the low-rank modeling helps in reducing the number of unknown variables, especially if the data are highly correlated. Then, the CPD factors of the two aggregated observations are

$$\underline{\mathbf{Y}}^t = \llbracket \mathbf{A}, \mathbf{B}, \mathbf{W}\mathbf{C} \rrbracket \quad (7)$$

$$\underline{\mathbf{Y}}^c = \llbracket \mathbf{U}\mathbf{A}, \mathbf{V}\mathbf{B}, \mathbf{C} \rrbracket \quad (8)$$

PREMA learns the factor matrices \mathbf{A}, \mathbf{B} , and \mathbf{C} by applying a coupled CPD model on the available aggregates with respect to the available observations. Figure 3 illustrates the high level picture of our model.

3.2 PREMA: Formulation

If we have the original (disaggregated) data in the tensor $\underline{\mathbf{X}}$ with missing entries, a common way to estimate its CPD factors is by adopting a least squares criterion to minimize the difference between the original tensor $\underline{\mathbf{X}}$ and its CPD factors $\llbracket \mathbf{A}, \mathbf{B}, \mathbf{C} \rrbracket$ with respect to the available (observed) entries. This can be done by adding a weight tensor that masks the available entries, i.e.,

$$\underset{\mathbf{A}, \mathbf{B}, \mathbf{C}}{\text{minimize}} \quad \|\underline{\Omega} \circledast (\underline{\mathbf{X}} - \llbracket \mathbf{A}, \mathbf{B}, \mathbf{C} \rrbracket)\|_F^2$$

where $\underline{\Omega}$ is defined as

$$\Omega(i, j, k) = \begin{cases} 1, & \text{if } \underline{\mathbf{X}}(i, j, k) \text{ is available} \\ 0, & \text{otherwise} \end{cases} \quad (9)$$

Fortunately, many real life data exhibit low-rankness due to the correlation between the elements within each dimension (e.g., stores, items, time stamps), i.e., R is small relative to the size of the tensor.

In the considered disaggregation task, we only have aggregated views of the multidimensional data (i.e., compressed version of the target tensor $\underline{\mathbf{X}}$). Oftentimes, these aggregated views have missing elements for various application-specific reasons such as privacy, lack of data collection, or absence of events. As mentioned earlier, an example of the absence of events is when an item was not offered in a specific store for a period of time. Setting the entry corresponding to this event to be 0 adds noise to the data since this item might have a large number of sales if it was offered. We use the fact that the aggregated tensors share the same factors (up to aggregation) as shown in equations (7) and (8) to jointly decompose $\underline{\mathbf{Y}}^t$ and $\underline{\mathbf{Y}}^c$ by means of coupled tensor factorization. To this end, and obtain the following formulation:

$$\underset{\mathbf{A}, \mathbf{B}, \mathbf{C}}{\min} \quad \mathcal{F} := \|\underline{\Omega}^t \circledast (\underline{\mathbf{Y}}^t - (\llbracket \mathbf{A}, \mathbf{B}, \mathbf{W}\mathbf{C} \rrbracket))\|_F^2 + \|\underline{\Omega}^c \circledast (\underline{\mathbf{Y}}^c - (\llbracket \mathbf{U}\mathbf{A}, \mathbf{V}\mathbf{B}, \mathbf{C} \rrbracket))\|_F^2 \quad (10)$$

where $\underline{\Omega}^t \in \{0, 1\}^{I \times J \times K_w}$ and $\underline{\Omega}^c \in \{0, 1\}^{I_u \times J_v \times K}$ are weight tensors with L_t, L_c ones respectively at the indices of the available entries of $\underline{\mathbf{Y}}^t$ and $\underline{\mathbf{Y}}^c$, respectively, and zeros elsewhere. As a result, the CPD factors \mathbf{A}, \mathbf{B} , and \mathbf{C} are learned with respect to the available data. One could add a regularization parameter λ to control the balance

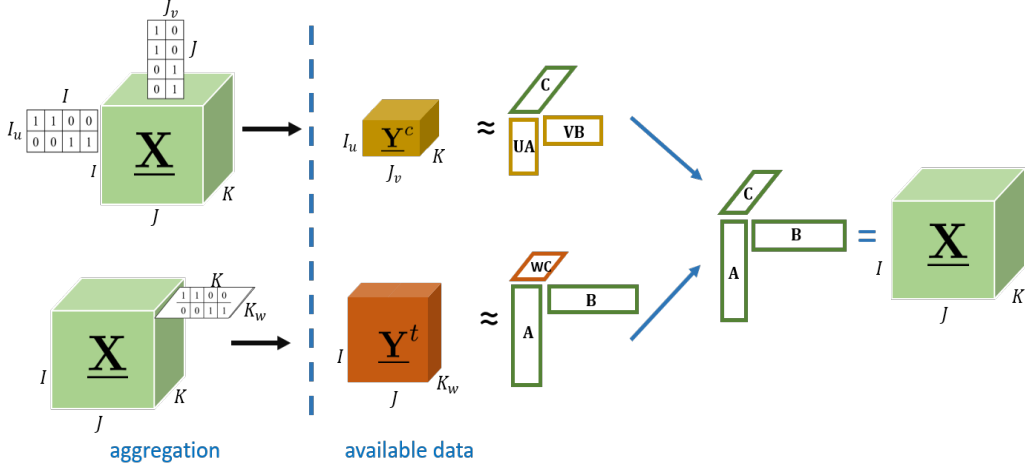


Fig. 3: Overview of PREMA.

between the two terms, however, we observe that it does not significantly affect the disaggregation performance. Note that if we have additional aggregated observations, we incorporate them using the same concept. Enforcing non-negativity constraints on the factors seems natural if we are dealing with count data, however, we empirically observed that it does not improve the disaggregation accuracy.

3.3 PREMA: Algorithm

The optimization in (10) is non-convex, and NP-hard in general. To tackle it, we employ a Block Coordinate Descent (BCD) algorithm to update the three variables in an alternating fashion. Starting from initial factors $\mathbf{A}^{(0)}$, $\mathbf{B}^{(0)}$, and $\mathbf{C}^{(0)}$, at every iteration $k \in \mathbb{N}$, we cyclically update each factor by fixing the other two. The update of \mathbf{A} can be written as:

$$\mathbf{A} \leftarrow \underset{\mathbf{A}}{\operatorname{argmin}} \mathcal{F} = \|\Omega_1^t \otimes (\mathbf{Y}_1^t - ((\mathbf{WC}) \odot \mathbf{B})\mathbf{A}^T)\|_F^2 + \|\Omega_1^c \otimes (\mathbf{Y}_1^c - (\mathbf{C} \odot (\mathbf{VB}))(\mathbf{UA})^T)\|_F^2$$

where \mathbf{Y}_1^t , \mathbf{Y}_1^c , Ω_1^t , and Ω_1^c are matrices resulting from mode-1 unfolding of their corresponding tensors. Let us define $\tilde{\mathbf{A}} = \mathbf{UA}$, $\tilde{\mathbf{B}} = \mathbf{VB}$, and $\tilde{\mathbf{C}} = \mathbf{WC}$ for convenience. By taking the partial derivative of the above objective function \mathcal{F} with respect to \mathbf{A} , we get the following equation—the derivations are deferred to Appendix A.

$$\frac{\partial \mathcal{F}}{\partial \mathbf{A}} = \nabla_{\mathbf{A}} \mathcal{F} = 2(\underbrace{\Omega_1^t \otimes ((\tilde{\mathbf{C}} \odot \mathbf{B})\mathbf{A}^T - \mathbf{Y}_1^t)}_{\mathbf{r}_t})^T (\tilde{\mathbf{C}} \odot \mathbf{B}) + 2\mathbf{U}^T (\underbrace{\Omega_1^c \otimes ((\mathbf{C} \odot \tilde{\mathbf{B}})\tilde{\mathbf{A}}^T - \mathbf{Y}_1^c)}_{\mathbf{r}_c})^T (\mathbf{C} \odot \tilde{\mathbf{B}}). \quad (11)$$

Similarly, we derive the derivatives of the \mathcal{F} with respect to \mathbf{B} and \mathbf{C} and get the following equations:

$$\nabla_{\mathbf{B}} \mathcal{F} = 2(\Omega_2^t \otimes ((\tilde{\mathbf{C}} \odot \mathbf{A})\mathbf{B}^T - \mathbf{Y}_2^t))^T (\tilde{\mathbf{C}} \odot \mathbf{A}) + 2\mathbf{V}^T (\Omega_2^c \otimes ((\mathbf{C} \odot \tilde{\mathbf{A}})\tilde{\mathbf{B}}^T - \mathbf{Y}_2^c))^T (\mathbf{C} \odot \tilde{\mathbf{A}}), \quad (12)$$

$$\nabla_{\mathbf{C}} \mathcal{F} = 2\mathbf{W}^T (\Omega_3^t \otimes ((\mathbf{B} \odot \mathbf{A})\tilde{\mathbf{C}}^T - \mathbf{Y}_3^t)) (\mathbf{B} \odot \mathbf{A}) + 2(\Omega_3^c \otimes ((\tilde{\mathbf{B}} \odot \tilde{\mathbf{A}})\mathbf{C}^T - \mathbf{Y}_3^c))^T (\mathbf{C} \odot \tilde{\mathbf{A}}) \quad (13)$$

With the above gradient expressions at hand, we have established the update direction for each block (factor), which is the negative gradient of \mathcal{F} with respect to each factor

$$\mathbf{A} = \mathbf{A} - \alpha^* \nabla_{\mathbf{A}} \mathcal{F}, \quad (14)$$

$$\mathbf{B} = \mathbf{B} - \beta^* \nabla_{\mathbf{B}} \mathcal{F}, \quad (15)$$

$$\mathbf{C} = \mathbf{C} - \gamma^* \nabla_{\mathbf{C}} \mathcal{F}. \quad (16)$$

We now seek to select the step-size terms α , β , and γ . We use the *exact line search* approach for this task. At every iteration $k \in \mathbb{N}$, α is chosen to minimize \mathcal{F} along the line $\{\mathbf{A} - \alpha \nabla_{\mathbf{A}} \mathcal{F} | \alpha \geq 0\}$

$$\underset{\alpha \geq 0}{\operatorname{argmin}} \mathcal{F}(\mathbf{A} - \alpha \nabla_{\mathbf{A}} \mathcal{F}) \quad (17)$$

Luckily, in our case, the above optimization can be solved optimally without extra heavy computations. The optimal solution to (17) is as follows (refer to Appendix B for derivations)

$$\alpha^* = \max(0, \frac{\mathbf{r}_t^T \mathbf{g}_t + \mathbf{r}_c^T \mathbf{g}_c}{\mathbf{g}_t^T \mathbf{g}_t + \mathbf{g}_c^T \mathbf{g}_c}), \quad (18)$$

where \mathbf{r}_t and \mathbf{r}_c are as defined in (33), and

$$\mathbf{g}_t = \operatorname{vec}(\Omega_1^t \otimes ((\tilde{\mathbf{C}} \odot \mathbf{B})\nabla_{\mathbf{A}} \mathcal{F}^T)), \quad (19)$$

$$\mathbf{g}_c = \operatorname{vec}(\Omega_1^c \otimes ((\mathbf{C} \odot \tilde{\mathbf{B}})(\mathbf{U}\nabla_{\mathbf{A}} \mathcal{F})^T)). \quad (20)$$

where $\operatorname{vec}(\cdot)$ is the vectorization operator. Note that $-\mathbf{r}_t$ and $-\mathbf{r}_c$ are already obtained when we compute the gradient in (33). We have also computed $(\tilde{\mathbf{C}} \odot \mathbf{B})$ and $(\mathbf{C} \odot \tilde{\mathbf{B}})$ in (33), which are needed to obtain \mathbf{g}_t and \mathbf{g}_c , respectively. Thus, the exact line search step only adds i) the multiplication of the transpose of the gradient $\nabla_{\mathbf{A}} \mathcal{F} \in \mathbb{R}^{I \times R}$ by a $K_w J \times R$ matrix (and $(\mathbf{U}\nabla_{\mathbf{A}} \mathcal{F})^T$ by $K J_v \times R$ matrix), and ii) the vectors inner multiplications in (18), which depends on the $\operatorname{nnz}(\mathbf{Y}^t)$ (and $\operatorname{nnz}(\mathbf{Y}^c)$).

In a similar fashion, β and γ are obtained by solving the following optimization functions:

$$\beta^* = \underset{\beta \geq 0}{\operatorname{argmin}} \mathcal{F}(\mathbf{B} - \beta \nabla_{\mathbf{B}} \mathcal{F}) \quad (21)$$

$$\gamma^* = \underset{\gamma \geq 0}{\operatorname{argmin}} \mathcal{F}(\mathbf{C} - \gamma \nabla_{\mathbf{C}} \mathcal{F}) \quad (22)$$

The solutions of the above (and their computational cost) are similar to the case of α , but with mode-2 and mode-3 tensor unfolding and rotating the factors. We provide a generic example of deriving the solution to (17), (21)-(22) in Appendix B. The overall steps of PREMA are summarized in Algorithm 1.

Algorithm 1 : PREMA

input: $\underline{\mathbf{Y}}^t, \underline{\mathbf{Y}}^c, \mathbf{U}, \mathbf{V}, \mathbf{W}, R$

Initialize: $\mathbf{A}, \mathbf{B}, \mathbf{C}, \tilde{\mathbf{A}}, \tilde{\mathbf{B}}, \tilde{\mathbf{C}}$

Repeat

- Update \mathbf{A} using (14), (33), and (18)
- Update \mathbf{A} using (15), (12), and (21)
- Update \mathbf{A} using (16), (13), and (22)

Until convergence criterion is met (max. #iteration)

output: $\mathbf{A}, \mathbf{B}, \mathbf{C}$

3.3.1 Initialization

We observed empirically that a careful initialization for the factors results in a better disaggregation accuracy and substantially reduces the operational time (i.e., reduces the required number of iterations). Thus, we propose to initialize for the factor matrices in PREMA based on CPD. Specifically, we perform CPD on one tensor to get two factors, then we solve a linear system using the other tensor to obtain the third factors. The missing entries are set to 0 when we compute the CPD and solve the linear system in the initialization step. If the contemporaneous aggregate $\underline{\mathbf{Y}}^c$ is aggregated in two dimensions, then we compute the CPD of $\underline{\mathbf{Y}}^t$ to get \mathbf{A}, \mathbf{B} , and $\tilde{\mathbf{C}}$. Then, we compute $\tilde{\mathbf{A}} = \mathbf{U}\mathbf{A}$ and $\tilde{\mathbf{B}} = \mathbf{V}\mathbf{B}$. Last, we solve the over-determined system

$$\mathbf{Y}_3^c = (\tilde{\mathbf{B}} \odot \tilde{\mathbf{A}})\mathbf{C}^T$$

to obtain \mathbf{C} . On the other hand, when $\underline{\mathbf{Y}}^t$ is only aggregated on the first dimension, i.e., $\mathbf{V} = \mathbf{I}$, then \mathbf{B} is common in the two aggregated tensors and we can use the CPD of either to compute two “disaggregated” factors. In this case, we use the tensor that its unaggregated dimension is larger; a detailed steps of the initialization are provided in Appendix C. We use the Matlab-based package `Tensorlab` to compute the CPD (e.g., `CPD(\underline{\mathbf{Y}}^c)`).

3.4 PREMA: Complexity Analysis

Regarding the complexity of PREMA, computing the khatri-Rao products required for computing the gradient w.r.t \mathbf{A} in (33) costs $\mathcal{O}(K_w J R + K J_v R)$, where R is the rank, which is usually small in real data as we will show in the experiments. The cost of the multiplication of the khatri-Rao product terms with \mathbf{r}_t and \mathbf{r}_c in (33) rely on $\text{nnz}(\underline{\mathbf{\Omega}}^t)$ and $\text{nnz}(\underline{\mathbf{\Omega}}^c)$, respectively, i.e., the number of observed entries in $\underline{\mathbf{Y}}^t$ and $\underline{\mathbf{Y}}^c$. Note that \mathbf{r}_c^T is also multiplied by the aggregation matrix \mathbf{U}^T from the left in (33), which is moderately sparse and therefore reduce the computational cost. The overall complexity for (33) is $\mathcal{O}((R(\text{nnz}(\underline{\mathbf{\Omega}}^t) + \text{nnz}(\underline{\mathbf{\Omega}}^c) + \max(K_w J I, K J_v I_u)))$). Following the same analysis, we can see that the complexity of computing the gradients w.r.t \mathbf{B} and \mathbf{C} are similar.

3.5 PREMA: Identifiability Analysis

After introducing the model and the algorithm, we establish identifiability of the PREMA model. As mentioned earlier, the multidimensional disaggregation task is an inverse ill-posed problem. Considering a low rank CPD model on the data, results in a tensor disaggregation problem with unique solution. In other words, the optimal solution of (10) is guaranteed to be unique, under mild conditions, and identify the original fine-resolution tensor almost surely. For the sake of simplicity we first assume that $\underline{\mathbf{Y}}^t$ doesn't have any missing values.

Proposition 1. Let $\underline{\mathbf{X}} \in \mathbb{R}^{I \times J \times K}$ be the target tensor to disaggregate with CPD $\underline{\mathbf{X}} = [\mathbf{A}, \mathbf{B}, \mathbf{C}]$ of rank R . Also let $\underline{\mathbf{Y}}^t \in \mathbb{R}^{I \times J \times K_w} = \underline{\mathbf{X}} \times_3 \mathbf{W}$ and $\underline{\mathbf{Y}}^c \in \mathbb{R}^{I_u \times J_v \times K} = \underline{\mathbf{\Omega}}^c \circledast (\underline{\mathbf{X}} \times_1 \mathbf{U} \times_2 \mathbf{V})$ be the two aggregated observations. Assume that \mathbf{A}, \mathbf{B} and \mathbf{C} are drawn from some absolutely continuous joint distribution with respect to Lebesgue measure in $\mathbb{R}^{(I \times J \times K)R}$, and that $(\mathbf{A}^*, \mathbf{B}^*, \mathbf{C}^*)$ is an optimal solution to problem (10). Also assume that the number of observed entries at each frontal slab of $\underline{\mathbf{Y}}^c$ is greater than or equal to R . Then, $\hat{\underline{\mathbf{X}}} = [\hat{\mathbf{A}}, \hat{\mathbf{B}}, \hat{\mathbf{C}}]$ disaggregates $\underline{\mathbf{Y}}^t, \underline{\mathbf{Y}}^c$ to $\underline{\mathbf{X}}$ almost surely if $R \leq \frac{1}{16} \min\{IJ, IK_w, JK_w, 16I_u J_v\}$.

The proof is intuitive and parallels recent results obtained in the hyperspectral imaging literature [41]. **Proof sketch:** We use Theorem 1 to claim identifiability of $\underline{\mathbf{Y}}^t$. Then factors \mathbf{A}, \mathbf{B} can be identified up to common permutation and scaling. The solution for \mathbf{C} is obtained via solving an overdetermined linear system of equations using $\underline{\mathbf{Y}}^c$. This way permutation and scaling is preserved and the target tensor is recovered as $\underline{\mathbf{X}} = [\mathbf{A}, \mathbf{B}, \mathbf{C}]$. In case where $\underline{\mathbf{Y}}^t$ has missing entries identifiability depends on the pattern of misses. Specifically, the results in [24], [25], [26] can be employed, when the available measurements are fiber, regularly or randomly sampled respectively. The conditions are more restrictive compared to the case of fully observed tensor, but guarantee identifiability of \mathbf{A}, \mathbf{B} up to common permutation and scaling. The solution for \mathbf{C} is the same as in the previous case. The detailed proof is presented in Appendix D.

3.6 B-PREMA: PREMA with Unknown Aggregation

In most practical applications the aggregation details are known. However, there exist cases with limited knowledge on how the data are aggregated, i.e., we do not know (or have partial knowledge of) \mathbf{U}, \mathbf{V} , and \mathbf{W} . We consider the case where each available aggregate is aggregated in one dimension, and propose the following formulation to get the factors of the disaggregated tensor (\mathbf{A}, \mathbf{B} , and \mathbf{C}):

$$\begin{aligned} \min_{\mathbf{A}, \mathbf{B}, \mathbf{C}, \tilde{\mathbf{A}}, \tilde{\mathbf{C}}} & \|\underline{\mathbf{\Omega}}^t \circledast (\underline{\mathbf{Y}}^t - [\mathbf{A}, \mathbf{B}, \tilde{\mathbf{C}}])\|_F^2 \\ & + \|\underline{\mathbf{\Omega}}^c \circledast (\underline{\mathbf{Y}}^c - [\tilde{\mathbf{A}}, \mathbf{B}, \mathbf{C}])\|_F^2 \end{aligned} \quad (23)$$

This problem is more challenging than (10) as the number of variables has been increased, with the same number of equations. In order to tackle it, we adopt an Alternating Optimization (AO) procedure described in Algorithm 2. All the updates in Algorithm 2 are closed form least squares solutions. To initialize the factors in Algorithm 2, we set

the missing entries to zeros, then we use Tensorlab and compute $(\text{CPD}(\mathbf{Y}^c))$ to get $\tilde{\mathbf{A}}$, $\tilde{\mathbf{B}}$, and $\tilde{\mathbf{C}}$. To get an initial estimate of $\tilde{\mathbf{C}}$, we sum every consecutive $w = \frac{K}{K_w}$ rows in \mathbf{C} . This way we approximate the temporal aggregation process in a very intuitive way, the true aggregation matrix being unknown¹. Note that in (23), there is an inherent scaling ambiguity between factors $\tilde{\mathbf{A}} - \mathbf{A}$, and $\tilde{\mathbf{C}} - \mathbf{C}$. Partial knowledge on a single aggregation matrix would automatically resolve this issue. However, we have observed that even for fully aggregation-agnostic scenarios our proposed approach achieves high quality disaggregation, as we will see next.

Algorithm 2 : B-PREMA

input: $\mathbf{Y}^t, \mathbf{Y}^c, R$

Initialize: $\tilde{\mathbf{A}}, \tilde{\mathbf{B}}, \tilde{\mathbf{C}} \leftarrow \text{CPD}(\mathbf{Y}^c)$

$\tilde{\mathbf{C}}(k_w, :) \leftarrow \sum_{k=w(k_w-1)+1}^{w \times k_w} \mathbf{C}(k, :)$

Repeat

- $\tilde{\mathbf{A}} \leftarrow \underset{\tilde{\mathbf{A}}}{\text{argmin}} \quad \|\mathbf{Y}_1^c - (\mathbf{C} \odot \tilde{\mathbf{B}}) \tilde{\mathbf{A}}^T\|_F^2$
- $\tilde{\mathbf{C}} \leftarrow \underset{\tilde{\mathbf{C}}}{\text{argmin}} \quad \|\mathbf{Y}_3^c - (\tilde{\mathbf{B}} \odot \tilde{\mathbf{A}}) \tilde{\mathbf{C}}^T\|_F^2$
- $\tilde{\mathbf{A}} \leftarrow \underset{\tilde{\mathbf{A}}}{\text{argmin}} \quad \|\mathbf{Y}_1^t - (\tilde{\mathbf{C}} \odot \tilde{\mathbf{B}}) \tilde{\mathbf{A}}^T\|_F^2$
- $\tilde{\mathbf{C}} \leftarrow \underset{\tilde{\mathbf{C}}}{\text{argmin}} \quad \|\mathbf{Y}_3^t - (\tilde{\mathbf{B}} \odot \tilde{\mathbf{A}}) \tilde{\mathbf{C}}^T\|_F^2$
- $\tilde{\mathbf{B}} \leftarrow \underset{\tilde{\mathbf{B}}}{\text{argmin}} \quad \|[\mathbf{Y}_2^t; \mathbf{Y}_2^c] - [(\tilde{\mathbf{C}} \odot \tilde{\mathbf{A}}); (\tilde{\mathbf{B}} \odot \tilde{\mathbf{A}})] \tilde{\mathbf{B}}^T\|_F^2$

Until convergence criterion is met (max. #iteration)

output: $\mathbf{A}, \mathbf{B}, \mathbf{C}$

4 EXPERIMENTAL DESIGN

In this section, we provide a detailed description of the setup we use in our experiments. First, we describe the data used in the experiments. Then, we explain the aggregation applied on data to generate aggregated views. Last, we present the baselines and evaluation metrics used for comparison.

4.1 Datasets

We evaluate PREMA using the following public datasets, which are readily available online:

DFF²: Retail sales data, called Dominick’s Finer Foods (DFF). These data were collected in partnership between DFF grocery store chain and the James M. Kilts Center, University of Chicago Booth School of Business for the purpose of academic research in shelf management and pricing. DFF used to be a grocery store chain based in the Chicago-area until all of its stores were closed. The DFF datasets are comprehensive and cover the weekly reported sales of more than 3,500 items for more than five years. Sales, in this dataset, are divided into category-specific files. In particular, each file contains the weekly sales (i.e., number of sold units) of items belonging to a specific category (e.g., cheese, soap, cookies, soft drinks, etc) in over 100 stores on a weekly basis. DFF data contain the geographical locations of the different stores.

1. In the experiments, we make sure that the true temporal aggregation (\mathbf{W}) and the estimated one do not align

2. <https://www.chicagobooth.edu/research/kilts/datasets/dominicks>

We create the groundtruth three-dimensional data (third-order tensor), using 10 different category-specific datasets. This way, a (stores \times items \times weeks) tensor $\mathbf{X} \in \mathbb{R}^{I \times J \times K}$ is formed for each category. We pick the 50 most popular items from each category. Note that this results in an ‘incomplete’ tensor, owing to the fact that not all items were offered in all stores, or they were only offered for part of the time for some stores. These tensors have varying statistics (see Table 2), which allows thorough testing and analysis.

Walmart³: Historical weekly sales data made available online for 45 Walmart stores located in different regions. These data contain the weekly sales for 99 departments. A (stores \times departments \times weeks) tensor is created from these data. The resulting tensor is complete and has no missing entries. The size of each store (in square feet) is included in the data (we use this information to form groups of stores).

Crime⁴: Reported incidents of crime that occurred in the city of Chicago from 2001 to present. Each incident is marked with its beat (police geographical area), and a code indicating the crime type. There are 304 geographical areas and 388 crime types in total. Using this data, we form a (locations (by beat) \times crime types \times months) tensor.

Weather⁵: Contain the daily weather observations from 49 weather stations in Australia. These observations contains 17 different variables, e.g., min temperature, max temperature, cloud, humidity, wind, etc. We form a (station (location) \times variables \times days) tensor from one year of daily observation.

Table 2 summarizes the different datasets described above with their size, maximum and average values, Standard Deviation (SD), and sparsity (percentage of missing entries). The first group, in the table, corresponds to ten department-specific datasets from DFF data—in the results we use the three bold letters acronym for these categories. The row under the department-specific datasets in Table 2 corresponds to the tensor that has items from all the 10 departments combined (called MIXed).

4.2 Aggregation Configuration

The aggregated observations (compressed tensors), that are used as inputs to the disaggregation methods, are generated from \mathbf{X} following two practical scenarios described below.

Scenario A: The multidimensional series, we aim to disaggregate, is represented by $\mathbf{X} \in \mathbb{R}^{I \times J \times K}$. Instead of the full tensor \mathbf{X} , we are given two aggregated views: 1) the point-of-sale or store-level data, where sales are aggregated over time and reported in temporal resolution lower than weekly (e.g., monthly, or quarterly), i.e., $\mathbf{Y}^t = \mathbf{X} \times_3 \mathbf{W}$, and 2) the weekly sales of groups of stores, aggregated together, i.e., $\mathbf{Y}^c = \mathbf{X} \times_1 \mathbf{U}$. We use the 10 categories datasets from DFF and Walmart data for this scenario. The stores are grouped according to their geographical locations in DFF, and based on their sizes in Walmart data. We also test this scenario on Weather data, where the temporal aggregate is the average weather observation averaged over a course of

3. <https://www.kaggle.com/c/walmart-recruiting-store-sales-forecasting/data>

4. <https://www.kaggle.com/chicago/chicago-crime/activity>

5. <http://www.bom.gov.au/climate/data/>

TABLE 2: Summary of datasets and their statistics.

Dataset (\underline{X})	Size	Max	Avg	SD	% (missing entries)	% (zero entries)
BATH Soap	93 × 50 × 266	52	0.79	1.34	44.73	33.37
Bottled JuiCes	93 × 50 × 393	12288	13.76	50.08	8.79	9.19
CHeeses	93 × 50 × 393	18176	26.65	88.29	8.59	5.51
COOkies	94 × 50 × 390	14080	16.00	56.86	9.81	7.57
CRAckers	94 × 50 × 382	14080	8.21	29.61	14.21	7.57
Canned SOup	93 × 50 × 379	34494	40.46	133.42	8.64	4.54
Fabric SoFteners	93 × 50 × 397	7168	5.68	18.84	18.64	27.48
GROoming	93 × 50 × 272	232	1.94	2.94	7.66	32.66
Paper ToWels	93 × 50 × 389	19712	45.36	117.82	36.72	23.49
Soft DRinks	93 × 50 × 391	18944	48.81	155.09	8.58	11.18
MIXed	93 × 500 × 230	17610	19.01	71.30	15.30	17.83
Walmart	45 × 99 × 143	6.93e+05	1.05e+04	1.99e+04	0	33.84
Crime	304 × 388 × 221	325	0.26	1.47	0	91.56
Weather	49 × 17 × 365	1038	10.23	95.65	0	93.30

time, and the contemporaneous aggregate is the average of the observations over a geographical region.

Scenario B: In this scenario, two aggregated views of \underline{X} are given: 1) similar to the pervious scenario, the temporally aggregated store-level sales $\underline{Y}^t = \underline{X} \times_3 \mathbf{W}$, and 2) the weekly sales reported that are *jointly* aggregated by groups of stores and groups of items $\underline{Y}^c = \underline{X} \times_1 \mathbf{U} \times_2 \mathbf{V}$. In the case of Crime data, these two aggregated tensors correspond to 1) the temporally aggregated crime incidents, and 2) incidents reported as aggregates over nearby locations and similar types of crimes, i.e., has lower resolution in the locations and types dimensions. Note that when $\mathbf{V} = \mathbf{I}$, this yields to Scenario A. The stores are aggregated into groups according to their geographical locations in MIX data, whereas, items are aggregated according to their categories. In Crime data, locations and types are grouped based on the closeness in geographical location and similarity in crime type, respectively. Evidently, this scenario is more challenging since the second observation is aggregated in two modes (stores and items, or locations and types), i.e., double aggregation, resulting in fewer available measurements.

The difficulty of the problem also depends on the *aggregation level*, i.e., the number of data points (e.g., weeks, items, or stores) in one sum. Fewer aggregated measurements result in more challenging problems from an “equations versus unknowns standpoint. We test the disaggregation performance using different aggregation levels for each dimension.

4.3 Evaluation Baselines & Metrics

We evaluate the disaggregation performance of the proposed method using the Normalized Mean Square Error (NMSE = $\|\underline{X} - \hat{\underline{X}}\|_F^2 / \|\underline{X}\|_F^2$), where $\hat{\underline{X}}$ is the estimated data. The baseline methods are described next. Note that we compare to state-of-art approaches in time series disaggregation literature as well as methods developed to fuse multiple views of multi-dimensional data, but for different tasks. To the best of our knowledge our work is the first to perform disaggregation on multidimensional data from multiple views.

Mean: For every entry in the target high-resolution data tensor, we have two aggregated samples (temporal and contemporaneous). Mean takes the average of these aggregated samples as the estimate of each entry. For example, suppose that 100 units of ice cream Z were sold in 10 stores for week 1 of January, and 80 Z ice creams were sold in January (4 weeks) at Store 1. Then, $\hat{\underline{X}}$ (Store 1, Z , Week 1)

= $(100/10 + 80/4)/2 = 15$. Mean simply assumes equal contributions of all the data points that formed a given sum. The performance of this naive baseline is a good indicator of how smooth the data are.

LS: This baseline is inspired by [19], [33], where a linear least squares criterion is adopted on the linear relationship between the target series in high resolution and the available aggregates. The resulting linear system is underdetermined, thus, these works assume a linear regression model between the target series and some set of indicators. In their context, indicators are time series available in high resolution that are expected to display similar fluctuations to the target series. For example, information on wages and salaries can be an indicator for compensation of employees. This assumption requires additional data that are not available in our datasets. Therefore, we resolve to the minimum norm solution to the linear system in this baseline. We explain this baseline with an example. Assume we have two types of cheese, c_1 and c_2 , offered in two stores, s_1 and s_2 . We are given two types of aggregated series: 1) the *monthly* sales of each type in each store (4 series in total, $y_{1,1}^t, y_{1,2}^t, y_{2,1}^t, y_{2,2}^t$), and 2) the *weekly* sales for both types in both stores collectively in one series y^c . To get the weekly sales for each type in each store ($x_{1,1}, x_{1,2}, x_{2,1}$, and $x_{2,2}$), We find the minimum norm solution to the following

$$\min_{\substack{x_{11}, x_{12}, \\ x_{21}, x_{22}}} \sum_{s,c=1}^2 \|y_{s,c}^t - \mathbf{W}x_{s,c}^t\|_2^2 + \|y^c - \sum_{s,c=1}^2 x_{s,c}\|_2^2 \quad (24)$$

Note that we solve for each group of stores and items that form one sum in \underline{Y}^c separately. The quality of the solution using this baseline is an indicator of how difficult the problem is, from an “equations versus unknowns” standpoint.

H-Fuse: [14] This baseline constrains the least squares solution to the linear relationship between the aggregated and disaggregated series (Eq. (24) in our case) to have a smooth solution, i.e., penalizes the large differences between adjacent time ticks. To simply the presentation, we use equation (6) as a trivial example. H-Fuse imposes the following soft constraint to the least squares criterion on the linear system in (6)

$$\left\| \underbrace{\begin{bmatrix} 1 & -1 & 0 & 0 & 0 \\ 0 & 1 & -1 & 0 & 0 \\ 0 & 0 & 1 & -1 & 0 \\ 0 & 0 & 0 & 1 & -1 \end{bmatrix}}_{\mathbf{H}} \begin{bmatrix} x_1 \\ x_2 \\ x_3 \\ x_4 \\ x_5 \end{bmatrix} \right\|_2^2 \quad (25)$$

HomeRun: [15] This baseline circumvents the underdeterminacy of the linear system in the time series disaggregation problem by solving for the disaggregated series in the frequency domain. More specifically, HomeRun searches for the coefficients of the Discrete Cosine Transform (DCT) that represent the target series. HomeRun also imposes smoothness and Non-Negativity (NN) constraints. Using the example in (6), HomeRun is formulated as follows

$$\begin{aligned} \underset{\mathbf{s}}{\operatorname{argmin}} \quad & \|\mathbf{s}\|_1 + 1/2\|\mathbf{H}\mathbf{D}^T\mathbf{s}\|_2^2 \\ \text{s.t.} \quad & \mathbf{U}\mathbf{D}^T\mathbf{s} = \mathbf{y}, \quad \mathbf{D}^T\mathbf{s} \geq \mathbf{0} \end{aligned} \quad (26)$$

where \mathbf{D} is the DCT basis matrix, $\mathbf{x} = \mathbf{D}^T\mathbf{s}$ (inverse DCT), $\mathbf{s} = \mathbf{D}\mathbf{x}$ (DCT), and \mathbf{H} is as defined in (25). Due to the l_1 norm criterion in (26), HomeRun is effective when the series can be well approximated using *few* DCT coefficients (i.e., quasi-periodic).

CMTF: Couple Matricized Tensor Factorization has been widely used to reconstruct a super-resolution image that has high resolution in both spatial and spectral domains by fusing two views, one has high spectral resolution but low spatial resolution, while the second has high spatial resolution but low spectral resolution [43], [44]—the work in [43] adds NN constraints. These images are three-dimensional tensors and the motivation behind these works is to exploit the low-rankness of the matricized images. We compare to this model because real world multidimensional series have low-rank as we will show empirically. Using our notation, CMTF solves

$$\begin{aligned} \min_{\mathbf{A}, \mathbf{B}} \quad & \|\Omega_3^t \otimes (\mathbf{Y}_3^t - \mathbf{A}(\mathbf{W}\mathbf{B})^T)\|_F^2 \\ & + \|\Omega_3^c \otimes (\mathbf{Y}_3^c - (\mathbf{V} \otimes \mathbf{U})\mathbf{A}\mathbf{B}^T)\|_F^2 \end{aligned} \quad (27)$$

where \otimes is the Kronecker product. We solve (27) using BCD algorithm with exact line search. Similar to PREMA, a good initialization guess for the low-rank factors improves the performance of CMTF. To ensure fair comparison, we initialize using SVD with missing entries set to be zeros.

In addition to the above baseline methods, we also test the estimation of the target series with the following *oracle* baseline.

CPD: We fit a CPD model directly to the ground-truth tensor $\underline{\mathbf{X}}$ with respect to the observed entries. We use the Matlab-based package `Tensorlab` to compute the CPD. Then we reconstruct $\hat{\underline{\mathbf{X}}}$ from the learned factors $(\mathbf{A}, \mathbf{B}, \mathbf{C})$ and measure the NMSE. This baseline can also serve as a lower bound for the error produced by the proposed PREMA.

5 EXPERIMENTAL RESULTS

In this section, we evaluate the performance of PREMA and B-PREMA in terms of disaggregation accuracy using real data. The two aforementioned aggregation scenarios (refer to Section 4.2) are considered at different aggregation levels. All experiments were performed using Matlab on a Linux server with an Intel Core i7-4790 CPU 3.60 GHz processor and 32 GB memory.

5.1 Results on Scenario A

Two aggregated views $\underline{\mathbf{Y}}^t, \underline{\mathbf{Y}}^c$ are observed. In $\underline{\mathbf{Y}}^t$, weekly sales are observed in a monthly basis, while in $\underline{\mathbf{Y}}^c$, the 93 (or 94 for some categories) stores are clustered geographically into 18 areas. This means that the measurements in the temporal aggregate $\underline{\mathbf{Y}}^t$ are about 25% of the original size, and the number of the contemporaneously aggregated measurements in $\underline{\mathbf{Y}}^c$ is only 19.35% of the disaggregated data size. Table 3 shows the disaggregation error, in terms of NMSE, achieved by the proposed method and the baselines on the 10 category-specific datasets from DFF data. The proposed method, PREMA and B-PREMA, are shown under 3 different ranks ($R = 10, R = 25, R = 40$). Whereas, For CMTF, we perform a grid search on the rank and show the best results.

For all datasets in Table 3, except BAT, PREMA markedly outperforms the baselines—to highlight the improvement, we make the smallest error in bold and underline the second smallest. The naive mean (Mean) is good enough with BAT dataset because it is smooth ($SD = 1.34$) and has the largest percentage of missing entries compared to the other datasets. The time series methods, H-Fuse and HomeRun, do not perform well with these datasets because they are designed for smooth and quasi-periodic data, respectively. To provide an example, we noticed that HomeRun improves the error of LS baseline with CRA data and found that CRA exhibit more periodicity compared to the rest of categories. Comparing PREMA with CPD, we see that PREMA achieves error very close to CPD of the ground-truth data with the same rank, e.g., with GRO, PTW, and SDR datasets. By looking at the performance of B-PREMA in the table, we can see that the proposed algorithm works remarkably well when the aggregation matrices are unknown. For example, with GRO data and $R = 40$, the NMSE of B-PREMA is 0.2509, while $NMSE = 0.2277$ for CPD. B-PREMA disaggregates with smaller, or very similar, error compared to the baselines that uses the aggregation pattern information—see results with CRA, FSF, GRO, and SDR datasets. With all datasets, there is always a wide range of R under which the proposed algorithm works similarly. This allows a good estimate of the rank from the CPD of available aggregated tensors ($\underline{\mathbf{Y}}^t$ and $\underline{\mathbf{Y}}^c$)—maximum rank of the aggregated tensors is a lower bound on the rank of the disaggregated tensor.

Next, we examine the performance of the proposed method and the baselines when we change the level of aggregation from moderate to very high. The disaggregation error is shown with two datasets from DFF data⁶, FSF and PTW, in Figure 4, and with Walmart and Weather⁷ datasets in Figure 5.

The aggregation levels in Figure 4 are: 1) monthly basis measurements (every 4 weeks) in $\underline{\mathbf{Y}}^t$, and the 93 stores are divided geographically into 18 areas (“mod agg”), and 2) quarterly samples (every 12 weeks) in $\underline{\mathbf{Y}}^t$, and the stores are divided into only 9 areas (“high agg”). We conclude from Figure 4 that PREMA is more robust with aggressive aggregation where only few samples are available.

6. We exclude LS, H-Fuse, and HomeRun from this comparison as they do not work well with these data.

7. HomeRun is excluded from results with Weather data as it has NN constraints.

TABLE 3: NMSE of the proposed methods and the baselines using the 10 category-specific datasets.

Dataset %missings SD	BAT (44.73%) 1.34	BJC (8.79%) 50.08	CHE (8.59%) 88.29	COO (9.81%) 56.86	CRA (14.21%) 29.61	CSO (8.64%) 133.42	FSF (18.64%) 18.84	GRO (7.66%) 2.94	PTW (36.72%) 117.82	SDR (8.58%) 155.09
Mean	0.3284	0.4441	0.3118	0.3596	0.5217	0.3309	0.5609	0.2464	0.2994	0.2860
LS	0.3328	0.6077	0.4650	0.6224	0.5889	0.4664	0.5982	0.2831	0.4593	0.5420
H-FUSE	0.3411	0.6437	0.4870	0.6414	0.5726	0.4885	0.6451	0.2863	0.4719	0.5644
HomeRun	0.3461	0.6453	0.4818	0.6284	0.5376	0.4856	0.6496	0.2877	0.4662	0.5594
CMTF	0.4254	0.1818	0.1954	0.1783	0.7455	0.1564	0.1930	0.2908	0.2577	0.1633
PREMA (R=10)	0.5134	0.1941	0.1742	0.1751	0.2591	0.1721	0.2008	0.3150	0.2790	0.1946
PREMA (R=25)	0.5113	0.1649	0.1494	0.1363	0.2524	0.1371	0.1788	0.2556	0.2139	0.1413
PREMA (R=40)	0.4882	0.1560	0.1450	0.1263	0.2601	0.1329	0.1738	0.2456	0.1938	0.1314
B-PREMA (R=10)	0.5371	0.3358	0.4183	0.2854	0.4025	0.2252	0.2191	0.3141	0.3820	0.2175
B-PREMA (R=25)	0.5988	0.4182	0.4432	0.2630	0.3036	0.2212	0.2101	0.2529	0.5656	0.2106
B-PREMA (R=40)	0.6090	0.3571	0.4145	0.2844	0.3565	0.2755	0.1921	0.2509	0.7417	0.2114
CPD (R=10)	0.4776	0.0937	0.0686	0.1203	0.0758	0.0797	0.0782	0.2900	0.2344	0.1328
CPD (R=25)	0.4335	0.0574	0.0413	0.0671	0.0506	0.0487	0.0495	0.2439	0.1344	0.0801
CPD (R=40)	0.4092	0.0435	0.0318	0.0534	0.0434	0.0338	0.0397	0.2277	0.1000	0.0595

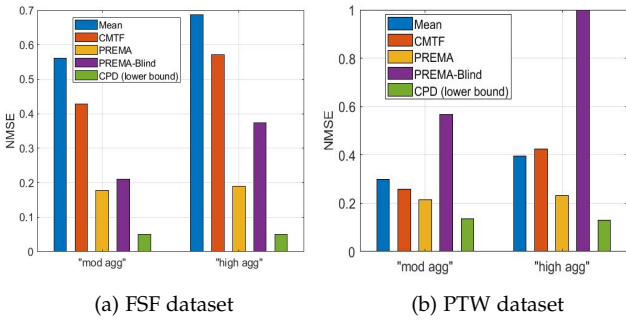


Fig. 4: PREMA works well with extreme aggregation.

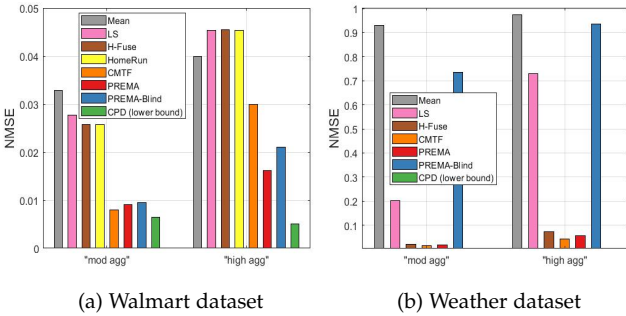


Fig. 5: PREMA works with different data.

For instance, with “high agg”, the number of aggregation samples is only 8.56% of the original size in the temporal aggregate, and 9.68% in the contemporaneous aggregate. In this case, the NMSE of the best baseline is 3.02 (1.17) \times the error of PREMA with FSF (PTW) dataset, respectively. Moreover, with no knowledge of the aggregation pattern, B-PREMA outperforms all baselines that have access to the aggregation information with FSF data. With PTW, B-PREMA does not perform well with high level of aggregation because it is given only very few samples as the sparsity of PTW is %36.72. B-PREMA works very well with data that are less sparse as we saw in Table 3.

With Walmart data in Figure 5 (a), “mod agg” means that weeks are aggregated into months in \mathbf{Y}^t , and the 45 stores are divided into 15 groups, whereas time is aggregated quarterly (12 weeks) and stores are clustered into 9 groups in “high agg”. CMTF works slightly better when the aggregation is moderate, owing to the fact that the second mode in Walmart data is departments as apposed to items from the same category. As a result, the advantage of tensor models over the matricized tensor in capturing the higher-order dependencies becomes less clear. However, PREMA is more immune to aggressive aggregation. In the “high level” case, PREMA disaggregate with NMSE that is 1.85 times smaller than the error of CMTF. Even without access to the aggregation information, B-PREMA reduced the error of the baselines.

In Figure 5 (b), “mod agg” corresponds to weekly samples of the mean of daily weather measurements, and the 49 stations are averaged into 13 stations. On the other hand, the daily measurements are averaged into monthly samples, and the 49 stations are clustered into 7 stations in the “high agg” case. PREMA, CMTF, and H-Fuse performs similarly with Weather data (it has 93.30% zeros) with moderate aggregation. The size of the second dimension of Weather data is 17, therefore, PREMA do not have advantage over CMTF. H-Fuse works well with this data as it penalizes the larger jumps between the adjacent time ticks (i.e., days), and weather data are well suited for such constraint.

5.2 Results on Scenario B

The contemporaneous aggregate \mathbf{Y}^c in this scenario is aggregated in two dimensions: stores and items with MIX data, or crime locations and types with Crime data⁸. We test this with three different aggregation levels with each data. Difficulty (i.e., level of aggregation), increases as we move from case (a) to (c)—Figure 6 shows the performance for these three cases.

With MIX data, these levels are: a) \mathbf{Y}^t aggregates weeks into monthly samples, while \mathbf{Y}^c groups the 93 stores into 18 areas with no aggregation over the items, b) samples in

8. LS, H-Fuse, and HomeRun are excluded from this comparison for the same reason.

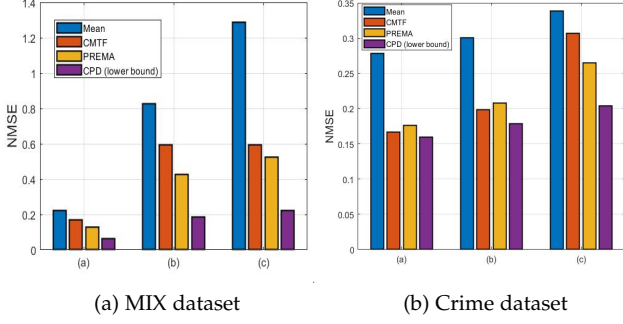


Fig. 6: PREMA works with double aggregation (Scenario B).

\mathbf{Y}^t has monthly resolution, and \mathbf{Y}^c groups the stores into 18 areas and items into groups of 10, and c) \mathbf{Y}^t contains temporal aggregates for each quarter, and \mathbf{Y}^c groups stores into 18 areas and items into groups of 25. One can see that the naive mean totally fails and its error exceeds 1 in case (c) with MIX data in Figure 6 (a). Notwithstanding, PREMA works well with double aggregation and few available samples.

With Crime data, the aggregation levels are: a) \mathbf{Y}^t aggregates the months into quarterly resolution, while \mathbf{Y}^c clusters both the crime locations and types into groups of 5, b) \mathbf{Y}^t has a quarterly time resolution, and \mathbf{Y}^c aggregates both the locations and types into groups of 10, and c) \mathbf{Y}^t aggregates the months into bi-yearly resolution, and \mathbf{Y}^c groups the crime locations and types into groups of 20. Figure 6 (b) shows the performance with these levels using Crime data. These data are challenging as they have 91.56% zero values and small SD, however, PREMA reduces the error of Mean. Although CMTF performs slightly better with the first two levels, PREMA becomes superior with harsh aggregation.

6 CONCLUSIONS

In this work, we proposed a novel framework, called PREMA, for fusing multiple aggregated views of multidimensional data. The proposed method leverages the properties of tensors in estimating the low-rank factors of the target data in higher resolution. The assumed model is provably transforming a highly ill-posed problem to an identifiable one. PREMA works with partially observed data and can disaggregate effectively without knowledge of the aggregation mechanism. Experimental results on real data show that the proposed algorithm is very effective, even with double aggregation and aggressive aggregation. The contributions of our work are summarized as follows:

- **Formulation:** we formally defined the problem of multidimensional data disaggregation from views aggregated in different dimensions.
- **Identifiability:** The considered tensor model provably converts a highly ill-posed problem to an identifiable one.
- **Effectiveness:** PREMA reduced the disaggregation error of the competing alternatives by up to 75%.
- **Scalability:** PREMA scales linearly with the data size in terms of run time.

- **Unknown aggregation:** B-PREMA works even when the aggregation mechanism is unknown.
- **Flexibility:** PREMA can disaggregate under the condition where data are partially observed.

APPENDIX A

DERIVATION OF GRADIENT EXPRESSIONS

We show the derivation of the gradient of one term that generalized the form of the two terms in (10). Consider the following function

$$\min_{\mathbf{A}, \mathbf{B}, \mathbf{C}} \mathcal{F} := \|\underline{\Omega} \circledast (\underline{\mathbf{Y}} - (\llbracket \mathbf{U}\mathbf{A}, \mathbf{V}\mathbf{B}, \mathbf{W}\mathbf{C} \rrbracket))\|_F^2 \quad (28)$$

Using mode-1 unfolding, (28) can be equivalently written as

$$\min_{\mathbf{A}, \mathbf{B}, \mathbf{C}} \mathcal{F} = \|\underline{\Omega}_1 \circledast (\mathbf{Y}_1 - (\mathbf{W}\mathbf{C} \circledast \mathbf{V}\mathbf{B})(\mathbf{U}\mathbf{A})^T)\|_F^2 \quad (29)$$

Vectorizing the above we get

$$\mathcal{F} = \|\mathbf{S}\mathbf{y} - \mathbf{S}(\mathbf{W}\mathbf{C} \circledast \mathbf{V}\mathbf{B} \circledast \mathbf{U}\mathbf{A})\mathbf{1}\|_F^2 \quad (30)$$

where \mathbf{S} is a diagonal selection matrix that has ones at the indices correspond to the available entries in \mathbf{y} , and zero elsewhere. (30) can be equivalently expressed as

$$\mathcal{F} = \|\mathbf{S}\mathbf{y} - \mathbf{S}(\mathbf{I} \otimes (\mathbf{W}\mathbf{C} \circledast \mathbf{V}\mathbf{B}))(\mathbf{U} \otimes \mathbf{I})\mathbf{a}\|_F^2 \quad (31)$$

We consider the derivative of \mathcal{F} w.r.t. \mathbf{A} (derivatives w.r.t. \mathbf{B} and \mathbf{C} are derived similarly by using mode-2 and mode-3 unfolding and rotating the factors accordingly).

$$\begin{aligned} \nabla_{\mathbf{A}} \mathcal{F} &= 2(\mathbf{U}^T \otimes \mathbf{I})(\mathbf{I} \otimes (\mathbf{W}\mathbf{C} \circledast \mathbf{V}\mathbf{B})^T) \mathbf{S}^T \mathbf{S} (\mathbf{I} \otimes (\mathbf{W}\mathbf{C} \circledast \mathbf{V}\mathbf{B}))(\mathbf{U} \otimes \mathbf{I})\mathbf{a} - 2(\mathbf{U}^T \otimes \mathbf{I})(\mathbf{I} \otimes (\mathbf{W}\mathbf{C} \circledast \mathbf{V}\mathbf{B})^T) \mathbf{S}^T \mathbf{S} \mathbf{y} \\ &= 2(\mathbf{I} \otimes (\mathbf{W}\mathbf{C} \circledast \mathbf{V}\mathbf{B})^T)(\mathbf{U}^T \otimes \mathbf{I}) \underbrace{\mathbf{S}^T \mathbf{S}}_{=\mathbf{S}} (\mathbf{I} \otimes (\mathbf{W}\mathbf{C} \circledast \mathbf{V}\mathbf{B}))(\mathbf{U} \otimes \mathbf{I})\mathbf{a} - 2(\mathbf{I} \otimes (\mathbf{W}\mathbf{C} \circledast \mathbf{V}\mathbf{B})^T)(\mathbf{U}^T \otimes \mathbf{I}) \mathbf{S}^T \mathbf{S} \mathbf{y} \\ &= 2(\mathbf{I} \otimes (\mathbf{W}\mathbf{C} \circledast \mathbf{V}\mathbf{B})^T)(\mathbf{U}^T \otimes \mathbf{I}) \mathbf{S} ((\mathbf{I} \otimes (\mathbf{W}\mathbf{C} \circledast \mathbf{V}\mathbf{B}))(\mathbf{U} \otimes \mathbf{I})\mathbf{a} - \mathbf{y}) \end{aligned} \quad (32)$$

Note that $(\mathbf{I} \otimes (\mathbf{W}\mathbf{C} \circledast \mathbf{V}\mathbf{B}))(\mathbf{U} \otimes \mathbf{I})$ is the tensor reconstructed using the estimated factors. Thus, it can be stated as $(\mathbf{W}\mathbf{C} \circledast \mathbf{V}\mathbf{B})(\mathbf{U}\mathbf{A})^T$ using mode-1 unfolding. Moreover, the multiplication of the vectorized tensors by \mathbf{S} in (32) is equivalent to the Hadamard product by $\underline{\Omega}_1$ in (29). As a result, using mode-1 unfolding, the final form in (32) can be written as

$$\nabla_{\mathbf{A}} \mathcal{F} = 2\mathbf{U}^T (\underline{\Omega}_1 \circledast ((\tilde{\mathbf{C}} \circledast \mathbf{B})\mathbf{A}^T - \mathbf{Y}_1))^T (\mathbf{W}\mathbf{C} \circledast \mathbf{V}\mathbf{B}) \quad (33)$$

This is a general results than can be applied directly in the case where only one or two modes are multiplied by an aggregation matrix.

APPENDIX B

DERIVATION OF STEP SIZE EXPRESSIONS

The step size terms are chosen using the exact line search optimization function. We show how to get the optimal solution of α as an example using the general formulation

in (28). It is easy to see how to get the solution when \mathcal{F} has more than one term as in this paper. α^* is obtained by solving

$$\alpha^* = \underset{\alpha \geq 0}{\operatorname{argmin}} \mathcal{F}(\mathbf{A} - \alpha \nabla_{\mathbf{A}} \mathcal{F}) \quad (34)$$

And equivalently,

$$\underset{\alpha \geq 0}{\operatorname{argmin}} \|\Omega_1 \otimes (\mathbf{Y}_1 - (\mathbf{W}\mathbf{C} \odot \mathbf{V}\mathbf{B})\mathbf{U}^T(\mathbf{A}^T - \alpha \nabla_{\mathbf{A}} \mathcal{F}))\|_F^2 \quad (35)$$

$$\underset{\alpha \geq 0}{\operatorname{argmin}} \underbrace{\|\Omega_1 \otimes (\mathbf{Y}_1 - (\mathbf{W}\mathbf{C} \odot \mathbf{V}\mathbf{B})\mathbf{U}^T \mathbf{A}^T)\|_F^2}_{\mathbf{E}} + \underbrace{\alpha \Omega_1 \otimes ((\mathbf{W}\mathbf{C} \odot \mathbf{V}\mathbf{B})\mathbf{U}^T \nabla_{\mathbf{A}} \mathcal{F}^T)}_{\mathbf{D}} \quad (36)$$

Respecting the non-negativity constraint, one can see that the optimal solution to the above is

$$\alpha = \max\left(0, \frac{-\operatorname{vec}(\mathbf{E})^T \operatorname{vec}(\mathbf{D})}{\operatorname{vec}(\mathbf{D})^T \operatorname{vec}(\mathbf{D})}\right), \quad (37)$$

APPENDIX C

INITIALIZATION ALGORITHM

The initialization steps of Algorithm 1 are as follows

set missing entries in $\underline{\mathbf{Y}}^t$, and $\underline{\mathbf{Y}}^c$ to zeros.

if $\mathbf{V} = \mathbf{I}$ then

if $K > I$ then

$\tilde{\mathbf{A}}, \mathbf{B}, \mathbf{C} \leftarrow \operatorname{CPD}(\underline{\mathbf{Y}}^c)$,

$\tilde{\mathbf{C}} = \mathbf{W}\mathbf{C}$,

$\mathbf{A} = ((\tilde{\mathbf{C}} \odot \mathbf{B})^\dagger \mathbf{Y}_1^t)^T$.

else

$\mathbf{A}, \mathbf{B}, \tilde{\mathbf{C}} \leftarrow \operatorname{CPD}(\underline{\mathbf{Y}}^t)$,

$\tilde{\mathbf{A}} = \mathbf{U}\mathbf{A}$,

$\mathbf{C} = ((\mathbf{B} \odot \tilde{\mathbf{A}})^\dagger \mathbf{Y}_3^c)^T$.

end if

else

$\tilde{\mathbf{A}}, \mathbf{B}, \tilde{\mathbf{C}} \leftarrow \operatorname{CPD}(\underline{\mathbf{Y}}^t)$,

$\tilde{\mathbf{A}} = \mathbf{U}\mathbf{A}$,

$\tilde{\mathbf{B}} = \mathbf{V}\mathbf{B}$,

$\mathbf{C} = ((\tilde{\mathbf{B}} \odot \tilde{\mathbf{A}})^\dagger \mathbf{Y}_3^c)^T$.

end if

where \mathbf{X}^\dagger is the MoorePenrose inverse of \mathbf{X} .

APPENDIX D

PROOF OF PROPOSITION 1

Let $\underline{\mathbf{X}} \in \mathbb{R}^{I \times J \times K}$ be the target tensor to disaggregate with CPD $\underline{\mathbf{X}} = \llbracket \mathbf{A}, \mathbf{B}, \mathbf{C} \rrbracket$ of rank R and $\underline{\mathbf{Y}}^t \in \mathbb{R}^{I \times J \times K_w} = \underline{\mathbf{X}} \times_3 \mathbf{W}$. Then under the conditions of Proposition 1, $\underline{\mathbf{Y}}^t$ admits a unique CPD $\underline{\mathbf{Y}}^t = \llbracket \mathbf{A}_t, \mathbf{B}_t, \mathbf{C}_t \rrbracket$. Since it is unique it holds that:

$$\mathbf{A}_t = \mathbf{A}\Pi\Lambda_1, \mathbf{B}_t = \mathbf{B}\Pi\Lambda_2, \mathbf{C}_t = \mathbf{W}\mathbf{C}\Pi\Lambda_3, \quad (38)$$

where Π is a permutation matrix and $\Lambda_1, \Lambda_2, \Lambda_3$ are diagonal matrices such that $\Lambda_1\Lambda_2\Lambda_3 = \mathbf{I}$. In the case where $\underline{\mathbf{Y}}^t$ has missing entries the conditions under which $\llbracket \mathbf{A}_t, \mathbf{B}_t, \mathbf{C}_t \rrbracket$ are identifiable are stricter and depend on the pattern of misses. We can use the conditions in [24], [25],

[26] for fiber, regular and random sampling respectively. So far factors \mathbf{A}, \mathbf{B} have been identified up to column permutation and scaling. What remains to be proven is that:

$$\underline{\Omega}^c \otimes \underline{\mathbf{Y}}^c = \underline{\Omega}^c \otimes (\underline{\mathbf{X}} \times_1 \mathbf{U} \times_2 \mathbf{V}) = \underline{\Omega}^c \otimes (\llbracket \mathbf{U}\mathbf{A}, \mathbf{V}\mathbf{B}, \mathbf{C} \rrbracket) \quad (39)$$

yields a solution for \mathbf{C}_c such that $\mathbf{C}_c = \mathbf{C}\Pi\Lambda_3$. Equation (39) can be equivalently written as:

$$\Omega_c \mathbf{y}_c = \Omega_c (\mathbf{C} \odot \mathbf{V}\mathbf{B} \odot \mathbf{U}\mathbf{A}) \mathbf{1} = \Omega_c (\mathbf{I} \otimes (\mathbf{V}\mathbf{B} \odot \mathbf{U}\mathbf{A})) \mathbf{c}, \quad (40)$$

where \mathbf{y}_c, \mathbf{c} are vectorized version of $\underline{\mathbf{Y}}^c, \mathbf{C}^T$ respectively and $\Omega_c \in \{0, 1\}^{L_c \times I_u J_v K}$ is a fat selection matrix, that selects the available entries of \mathbf{y}_c .

Now let $\tilde{\mathbf{A}} = \mathbf{U}\mathbf{A}$ and $\tilde{\mathbf{B}} = \mathbf{V}\mathbf{B}$. Following [41, Lemma 1] $\tilde{\mathbf{A}}, \tilde{\mathbf{B}}$ are drawn from absolutely continuous non-singular distributions. Also let $\mathbf{P} = \tilde{\mathbf{B}} \odot \tilde{\mathbf{A}}$. Since $I_u J_v \geq R$ the determinant of any $R \times R$ submatrix of \mathbf{P} is a non-trivial analytic function of $\tilde{\mathbf{A}}, \tilde{\mathbf{B}}$. Therefore any $R \times R$ minor of \mathbf{P} is non-zero almost surely [45, Lemma 3] and any R rows of \mathbf{P} are independent.

Taking a closer look at matrix $\mathbf{G} = \mathbf{I} \otimes (\mathbf{V}\mathbf{B} \odot \mathbf{U}\mathbf{A}) = \mathbf{I} \otimes (\tilde{\mathbf{B}} \odot \tilde{\mathbf{A}})$ we observe that it is an $I_u J_v K \times KR$ block diagonal matrix of the form:

$$\mathbf{G} = \begin{bmatrix} \mathbf{P} & \mathbf{0} & \dots & \mathbf{0} \\ \mathbf{0} & \mathbf{P} & \dots & \mathbf{0} \\ \vdots & \vdots & \ddots & \vdots \\ \mathbf{0} & \mathbf{0} & \dots & \mathbf{P} \end{bmatrix} = \begin{bmatrix} \mathbf{G}_1 \\ \mathbf{G}_2 \\ \vdots \\ \mathbf{G}_K \end{bmatrix} \quad (41)$$

Each block \mathbf{G}_k corresponds to the k -th frontal slab of $\underline{\mathbf{Y}}^c$ and the rows between different \mathbf{G}_k 's are independent by construction. Since we have assumed that the minimum number of observed entries for each frontal slab is greater or equal to R , then $\Omega_c \mathbf{G}$ has full column rank equal to KR and the solution for \mathbf{c} in (42) is unique with probability 1. Plugging $\mathbf{A}_t, \mathbf{B}_t$ in equation (42) we get:

$$\Omega_c \mathbf{y}_c = \Omega_c (\mathbf{C} \odot \mathbf{V}\mathbf{B}_t \odot \mathbf{U}\mathbf{A}_t) \mathbf{1} \quad (42)$$

$$= \Omega_c (\mathbf{C} \odot \mathbf{V}\mathbf{B}\Pi\Lambda_2 \odot \mathbf{U}\mathbf{A}\Pi\Lambda_1) \mathbf{1} \quad (43)$$

Then the unique solution for \mathbf{C} satisfies $\mathbf{C}_c = \mathbf{C}\Pi\Lambda_3$ and $\hat{\underline{\mathbf{X}}} = \llbracket \mathbf{A}_t, \mathbf{B}_t, \mathbf{C}_c \rrbracket$ disaggregates $\underline{\mathbf{Y}}^t, \underline{\mathbf{Y}}^c$ to $\underline{\mathbf{X}}$ almost surely.

REFERENCES

- [1] A. Silvestrini and D. Veredas, "Temporal aggregation of univariate and multivariate time series models: a survey," *J. of Econ. Surveys*, vol. 22, no. 3, pp. 458–497, 2008.
- [2] S. Uludag, K.-S. Lui, K. Nahrstedt, and G. Brewster, "Analysis of topology aggregation techniques for qos routing," *ACM Computing Surveys (CSUR)*, vol. 39, no. 3, p. 7, 2007.
- [3] N. S. Patil and P. Patil, "Data aggregation in wireless sensor network," in *IEEE intl conf. on comput. intell. and computing research*, vol. 6, 2010.
- [4] E. Shi, H. Chan, E. Rieffel, R. Chow, and D. Song, "Privacy-preserving aggregation of time-series data," in *Annual Network & Distributed System Security Symposium (NDSS)*. Internet Society, 2011.
- [5] Y. Park and J. Ghosh, "Ludia: An aggregate-constrained low-rank reconstruction algorithm to leverage publicly released health data," in *Proc. of the 20th ACM SIGKDD intl. conf. on Knowledge discovery and data mining*. ACM, 2014, pp. 55–64.
- [6] R. H. Ellaway, M. V. Pusic, R. M. Galbraith, and T. Cameron, "Developing the role of big data and analytics in health professional education," *Medical teacher*, vol. 36, no. 3, pp. 216–222, 2014.
- [7] I. Motakis and C. Zaniolo, "Temporal aggregation in active database rules," in *Proc. of the 1997 ACM SIGMOD Intl. Conf. on Mgmt. of Data*, ser. SIGMOD '97, 1997, pp. 440–451.

- [8] Z. Erkin, J. R. Troncoso-Pastoriza, R. L. Lagendijk, and F. Pérez-González, "Privacy-preserving data aggregation in smart metering systems: An overview," *IEEE Signal Process. Mag.*, vol. 30, no. 2, pp. 75–86, 2013.
- [9] W. A. Clark and K. L. Avery, "The effects of data aggregation in statistical analysis," *Geo. Analysis*, vol. 8, no. 4, pp. 428–438, 1976.
- [10] T. A. Garrett, "Aggregated versus disaggregated data in regression analysis: implications for inference," *Economics Letters*, vol. 81, no. 1, pp. 61–65, 2003.
- [11] Y. Jin, B. D. Williams, M. A. Waller, and A. R. Hofer, "Masking the bullwhip effect in retail: the influence of data aggregation," *Intl. J. of Physical Distrib. & Logistics Mgmt.*, vol. 45, no. 8, pp. 814–830, 2015.
- [12] M. Lenzen, "Aggregation versus disaggregation in input–output analysis of the environment," *Econ. Sys. Research*, vol. 23, no. 1, pp. 73–89, 2011.
- [13] D. Cole, "The effects of student-faculty interactions on minority students' college grades: Differences between aggregated and disaggregated data." *J. of the Professoriate*, vol. 3, no. 2, 2010.
- [14] Z. Liu, H. A. Song, V. Zadorozhny, C. Faloutsos, and N. Sidiropoulos, "H-fuse: Efficient fusion of aggregated historical data," in *Proc. of the 2017 SIAM Int. Conf. on Data Mining*, Houston, Texas, USA, April 2017, pp. 786–794.
- [15] F. M. Almutairi, F. Yang, H. A. Song, C. Faloutsos, N. Sidiropoulos, and V. Zadorozhny, "Homerun: scalable sparse-spectrum reconstruction of aggregated historical data," *Proc. of the VLDB Endowment*, vol. 11, no. 11, pp. 1496–1508, 2018.
- [16] N. Rossi *et al.*, "A note on the estimation of disaggregate time series when the aggregate is known," *The Review of Econ. and Stats.*, vol. 64, no. 4, pp. 695–696, 1982.
- [17] G. C. Chow and A.-I. Lin, "Best linear unbiased interpolation, distribution, and extrapolation of time series by related series," *The review of Econ. and Stats.*, pp. 372–375, 1971.
- [18] J. M. Pavía-Miralles, "A survey of methods to interpolate, distribute and extra-polate time series," *J. of Service Science and Mgmt. anagement*, vol. 3, no. 04, p. 449, 2010.
- [19] J. M. Pavía-Miralles and B. Cabrer-Borrás, "On estimating contemporaneous quarterly regional gdp," *J. of Forecasting*, vol. 26, no. 3, pp. 155–170, 2007.
- [20] B. D. Williams and M. A. Waller, "Creating order forecasts: point-of-sale or order history?" *J. of Business Logistics*, vol. 31, no. 2, pp. 231–251, 2010.
- [21] Y. H. Jin, B. D. Williams, T. Tokar, and M. A. Waller, "Forecasting with temporally aggregated demand signals in a retail supply chain," *Journal of Business Logistics*, vol. 36, no. 2, pp. 199–211, 2015.
- [22] F. L. Hitchcock, "The expression of a tensor or a polyadic as a sum of products," *Journal of Mathematics and Physics*, vol. 6, no. 1-4, pp. 164–189, 1927.
- [23] L. Chiantini and G. Ottaviani, "On generic identifiability of 3-tensors of small rank," *SIAM J. on Matrix Analysis and App.*, vol. 33, no. 3, pp. 1018–1037, 2012.
- [24] M. Sørensen and L. De Lathauwer, "Fiber sampling approach to canonical polyadic decomposition and application to tensor completion," *SIAM Journal on Matrix Analysis and Applications*, vol. 40, no. 3, pp. 888–917, 2019.
- [25] C. I. Kanatsoulis, X. Fu, N. D. Sidiropoulos, and M. Akçakaya, "Tensor completion from regular sub-nyquist samples," *arXiv preprint arXiv:1903.00435*, 2019.
- [26] M. Ashraphijuo and X. Wang, "Fundamental conditions for low-rp-rank tensor completion," *The Journal of Machine Learning Research*, vol. 18, no. 1, pp. 2116–2145, 2017.
- [27] N. D. Sidiropoulos, L. De Lathauwer, X. Fu, K. Huang, E. E. Papalexakis, and C. Faloutsos, "Tensor decomposition for signal processing and machine learning," *IEEE Transactions on Signal Processing*, vol. 65, no. 13, pp. 3551–3582.
- [28] T. G. Kolda and B. W. Bader, "Tensor decompositions and applications," *SIAM review*, vol. 51, no. 3, pp. 455–500, 2009.
- [29] M. Lenzerini, "Data integration: A theoretical perspective," in *Proc. of the 21st ACM SIGMOD-SIGACT-SIGART symposium on Princ. of database sys.* ACM, 2002, pp. 233–246.
- [30] X. L. Dong and F. Naumann, "Data fusion: resolving data conflicts for integration," *Proc. of the VLDB Endowment*, vol. 2, no. 2, pp. 1654–1655, 2009.
- [31] C. Faloutsos, H. V. Jagadish, and N. Sidiropoulos, "Recovering information from summary data," *PVLDB*, vol. 1, no. 1, pp. 36–45, 1997.
- [32] C. Sax and P. Steiner, "Temporal disaggregation of time series," *The R Journal*, vol. 5, no. 2, pp. 80–87, 2003.
- [33] T. Di Fonzo, "The estimation of m disaggregate time series when contemporaneous and temporal aggregates are known," *The Rev. of Econ. and Stats.*, pp. 178–182, 1990.
- [34] H.-F. Yu, N. Rao, and I. S. Dhillon, "Temporal regularized matrix factorization for high-dimensional time series prediction," in *Advances in neural information processing systems*, 2016, pp. 847–855.
- [35] Y. Matsubara, Y. Sakurai, C. Faloutsos, T. Iwata, and M. Yoshikawa, "Fast mining and forecasting of complex time-stamped events," in *Proc. of the 18th ACM SIGKDD intl. conf. on Knowl. discovery and data mining.* ACM, 2012, pp. 271–279.
- [36] K. Takeuchi, H. Kashima, and N. Ueda, "Autoregressive tensor factorization for spatio-temporal predictions," in *2017 IEEE Intl. Conf. on Data Mining (ICDM).* IEEE, 2017, pp. 1105–1110.
- [37] F. M. Almutairi, N. D. Sidiropoulos, and G. Karypis, "Context-aware recommendation-based learning analytics using tensor and coupled matrix factorization," *IEEE Journal of Selected Topics in Signal Processing*, vol. 11, no. 5, pp. 729–741, 2017.
- [38] E. E. Papalexakis, C. Faloutsos, and N. D. Sidiropoulos, "Tensors for data mining and data fusion: Models, applications, and scalable algorithms," *ACM Trans. Intell. Syst. Technol.*, vol. 8, no. 2, pp. 16:1–16:44, Oct. 2016.
- [39] C. I. Kanatsoulis, X. Fu, N. D. Sidiropoulos, and W.-K. Ma, "Hyperspectral super-resolution: Combining low rank tensor and matrix structure," in *2018 25th IEEE International Conference on Image Processing (ICIP).* IEEE, 2018, pp. 3318–3322.
- [40] —, "Hyperspectral super-resolution via coupled tensor factorization: Identifiability and algorithms," in *2018 IEEE International Conference on Acoustics, Speech and Signal Processing (ICASSP).* IEEE, 2018, pp. 3191–3195.
- [41] C. I. Kanatsoulis, X. Fu, N. D. Sidiropoulos, and W. Ma, "Hyperspectral super-resolution: A coupled tensor factorization approach," *IEEE T. on Signal Process.*, vol. 66, no. 24, pp. 6503–6517, Dec 2018.
- [42] C. I. Kanatsoulis, N. D. Sidiropoulos, M. Akçakaya, and X. Fu, "Regular sampling of tensor signals: Theory and application to fmri," in *ICASSP 2019-2019 IEEE International Conference on Acoustics, Speech and Signal Processing (ICASSP).* IEEE, 2019, pp. 2932–2936.
- [43] N. Yokoya, T. Yairi, and A. Iwasaki, "Coupled nonnegative matrix factorization unmixing for hyperspectral and multispectral data fusion," *IEEE Transactions on Geoscience and Remote Sensing*, vol. 50, no. 2, pp. 528–537, 2011.
- [44] M. Simões, J. Bioucas-Dias, L. B. Almeida, and J. Chanussot, "A convex formulation for hyperspectral image superresolution via subspace-based regularization," *IEEE Transactions on Geoscience and Remote Sensing*, vol. 53, no. 6, pp. 3373–3388, 2014.
- [45] R. C. Gunning and H. Rossi, *Analytic functions of several complex variables.* American Mathematical Soc., 2009, vol. 368.